University of Cincinnati

Date: 2/17/2011

<u>I, Ronnie A Mathew M.S., hereby submit this original work as part of the requirements for the degree of Master of Science in Mechanical Engineering.</u>

It is entitled:

Study of the Pulsed Electrochemical Micromachining of Ultra High Aspect Ratio Micro Tools

Student's name: **Ronnie A Mathew M.S.**

This work and its defense approved by:

Committee chair: Murali Sundaram, PhD

Committee member: Sundararaman Anand, PhD

Committee member: David Thompson, PhD

1374

Study of the Pulsed Electrochemical Micromachining of Ultra High Aspect Ratio Micro Tools

A thesis submitted to the

Graduate School

of the University of Cincinnati

in partial fulfillment of the

requirements for the degree of

Master of Science

in the Department of Mechanical Engineering

of the College of Engineering & Applied Sciences

by

Ronnie Mathew

Bachelor of Technology (B.Tech.)

National Institute of Technology Karnataka, Surathkal, India

May 2008

Committee Chair: Dr. Murali Sundaram

ABSTRACT

High aspect ratio metallic cylindrical rods having diameters in the sub millimeter range are increasingly being used as micro tools to machine complex micro features including deep hole micro drilling in a wide variety of engineering materials including metals and ceramics. They are also being used in applications such as ultrafine micro needles for intracellular sensing probes and micro robotic manipulators. Accurate and precise micro tools are essential for the micromachining of these highly complex features. Micro tools produced by the well known wire electro-discharge grinding suffer deformation due to the thermal stresses. Therefore, electrochemical machining has been explored as an alternate micro tool manufacturing technique. In this thesis, a micro electrochemical machining system has been designed and built in-house and a mathematical model has been developed to predict the final diameter of the anode based on the velocity of the cathode movement. Experimental verification of the model reveals good correlation with theoretical predictions. Large pulse on-times have successfully been used to fabricate micro tools having diameters of 10 micrometers with aspect ratios as high as 450. Pulse on-time between 5 to 10 ms was found to be an optimum range for successful micromachining using the in-house built micro electrochemical system. Pulse on-times lower than this optimum range result in a conical shape while pulse on-times higher than the optimum range result in a reverse conical shape.

ACKNOWLEDGEMENTS

I would like to thank my advisor Dr Murali Sundaram who has been more than a mentor for me and has shown me the path to achieving my goals. Dr. Sundaram has always emphasized on thinking outside the box and putting in a lot of hard work into research area in order to yield exceptional results. I will be ever grateful for all the help and knowledge I have received from him. My deepest thanks go to Dr. Sam Anand who guided and supported me especially through my first year of study at the University of Cincinnati. I would also like to thank Dr. David Thompson for imparting his knowledge and guidance through my graduate studies. I would also like to thank all of them for serving in my thesis defense committee.

I would also like to thank all my colleagues in the Micro and Nano Manufacturing Lab for their constant suggestions, ideas and criticisms. I would specifically like to thank Sagil James and Abishek Kamaraj, with whom I got the opportunity to research with. A big shout of thanks also goes to all my friends from other research areas in the University of Cincinnati who helped me in so many ways.

I would finally thank University of Cincinnati for giving me this opportunity to pursue my Masters of Science with a financial assistance and also do some amazing research.

TABLE OF CONTENTS

LIST OF FIGURES

LIST OF TABLES

LIST OF NOTATIONS / NOMENCLATURE

A	Atomic weight
D_f	final diameter of the tool electrode (m)
D_i	initial diameter of the tool electrode (m)
F	Faraday's constant ($C.mol^{-1}$)
k_v	volumetric electrochemical equivalent (m^3/As)
m	mass of metal removed or deposited (g)
p	pulse rate (1/s)
r_a	anodic dissolution rate (m/s)
S	interelectrode gap (m)
S_0	initial interelectrode gap (m)
t_p	pulse on-time (s)
U_0	applied voltage (V)
V	velocity of cathode (m/s)
W	width of cathode (m)
z	valency
ΔU	over potential (V)
η	current efficiency
κ_e	electrolyte conductivity (A/V m)

CHAPTER 1

1. Introduction

Product miniaturization has become an established trend in manufacturing due to multiple benefits including cost and material savings. Consequently, the products at micro level have gained significant interest among consumers. Micro components are being used in several important daily life products such as watches and electronic equipment. Silicon as a material has been used extensively in the electronics industry. It is the most popular material used in microelectromechanical systems (MEMS) devices [1]. However, silicon manufacturing as a technology has intrinsic limitations of fabrication of true 3D micro mechanisms [2]. It also has disadvantages in applications that demand higher stress, torque or have specific temperature requirements [3]. Alternatives to silicon are several high strength engineering alloys and metals. These high strength alloys however, are hard to micromachine using traditional manufacturing processes moreover, existing lithographic techniques are also not suitable to micromachine these advanced engineering materials. Nontraditional manufacturing processes are required to overcome these micromachining challenges [4, 5].

Electrochemical Machining (ECM) is a non-traditional manufacturing which uses electric current to pass through an electrolyte flowing between a tool (cathode) and a work piece (anode) thus using anodic dissolution to form the components [6, 7]. ECM of micro sized features or ‘micro ECM’ has several applications in commercial sectors such as biomedical industry, automobile industry, painting and coating industry, cosmetic industry etc [8].

1.1. Motivation of Research

With the outbreak of product miniaturization, more complex manufacturing challenges have emerged such as deep hole drilling for applications such as fuel injectors and lubricating holes. Accurate and precise high aspect ratio metallic micro tools are required to conduct micromachining for such applications. Aspect ratio for a tool is defined as the length of the tool divided by the diameter of the tool. Other applications of high aspect ratio structures include ultrafine micro needles for minimal invasive brain sensors and micro robotic manipulators.

Wire electro discharge grinding (WEDG) and micro electrodischarge machining (EDM) are two well known processes to manufacture micro tools. EDM is a process in which the material is removed by means of a series of repeated electrical discharges applied between the anode and the cathode in the presence of a dielectric fluid [9, 10]. WEDG is basically a variation of the EDM process where the tool is a wire electrode and its path is supported by a wire electrode traveling system and a positioning system [11]. However, the WEDG process suffers from drawbacks such as surface deformation, tool wear and residual stresses [11, 12]. Tensile stresses generated in the re-solidified layer cause structural deformation especially in really thin edged surfaces as seen in figure 1 due to residual stresses [13]. In micro EDM, surface cracks are formed on the electrode surface machined as shown in figure 2 due to tensile stresses developed from different solidification times of the various layers [14]. These cracks can also grow into holes because of the high stress concentration at those regions. Therefore, it is necessary to find alternate processes that are capable of micro tool manufacturing without the above mentioned drawbacks.

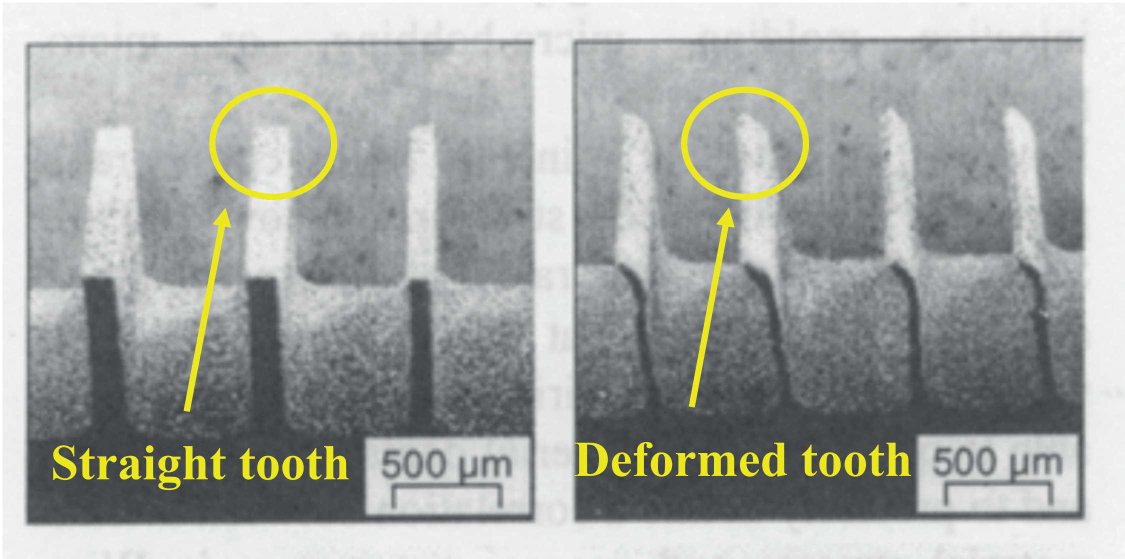

Figure 1 - Tooth Deviation due to tensile residual Stresses [13]

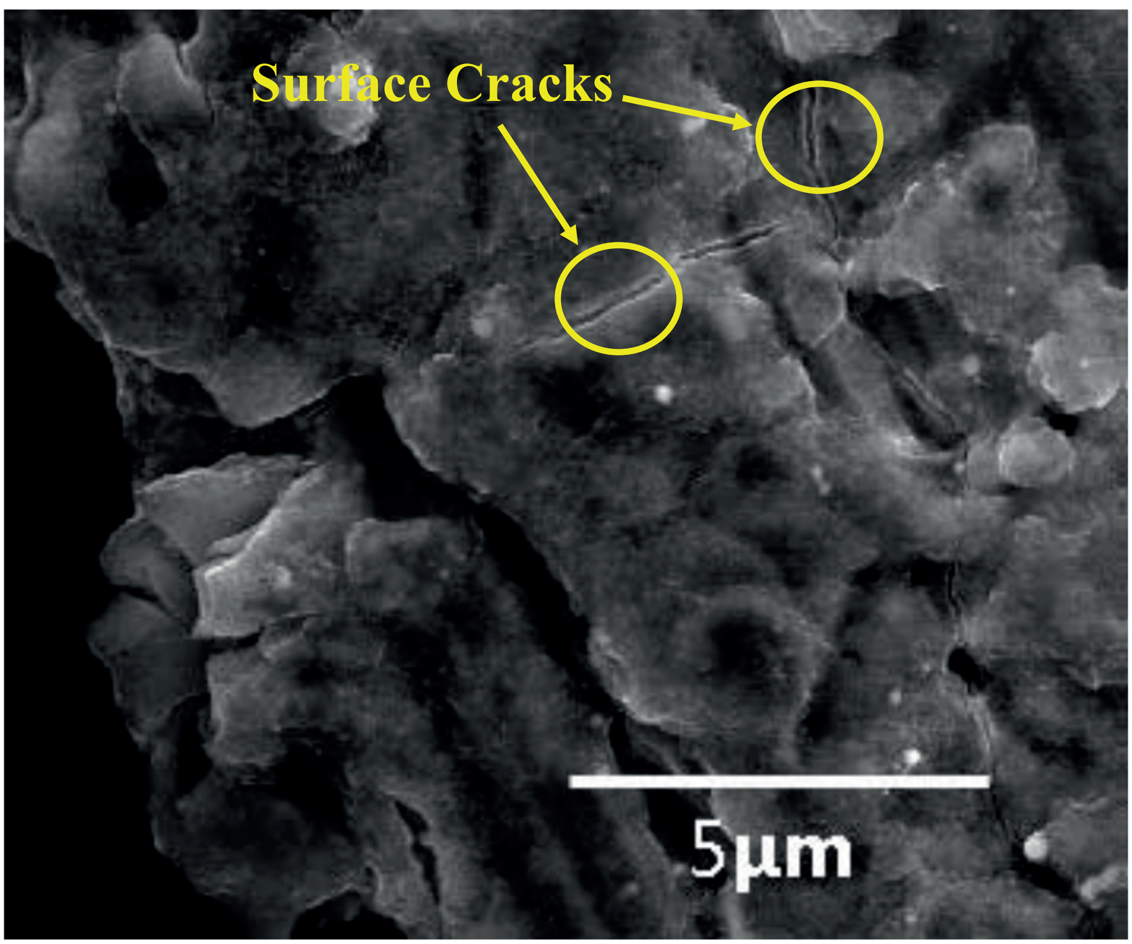

Figure 2 - Surface Cracks appearing on the micro tool machined by EDM [14]

Electrochemical machining (ECM) is a potential method to overcome the thermal effects seen in EDM and WEDG. ECM is basically a controlled anodic electrochemical dissolution process in an electrolytic cell during an electrolysis process [7, 15]. The anodic dissolution taking place is used to machine the components. Some of the advantages of ECM are: its independence of the hardness of the material being machined, no tool wear, and a relatively high machining rate [7, 16-18]

High aspect ratio micro tools have several applications such as in the fabrication of lubrication holes in powertrain components, holes in injection nozzles and fuel injectors in automobiles and cooling holes in jet or gas turbines [19]. They also have potential application in the fabrication of the wings of micro air vehicles [20]. As a probe, they have large applications as intracellular sensing probes in the biomedical industry [21]. They also have applications in the painting and coating industry, cosmetic industry etc [8].

Continuous efforts are being made to improve the process capabilities of micromachining. Some of the recent researches have been focused on making micro structures with higher aspect ratios using micromachining processes. LIGA (Lithographie, Galvanoformung, Abformung) process is one of the popular methods to make high aspect ratio structures [22]. However, this process suffers from several drawbacks including high fabrication costs and restricted choice of work materials [23]. Micro ECM is a potential alternative to achieve micro structures with higher aspect ratios.

1.2. Objective

The objective of this research is to study the effect of the velocity of the cathode and pulse on-time on the anodic profile of the resulting tool electrode and fabricate ultra high aspect ratio micro tools using micro ECM process.

1.3. Outline of thesis

The thesis is organized as follows: the introduction in Chapter 1 is followed by a detailed literature review of relevant research works in Chapter 2. Chapter 3 discusses the system design of the in-house built micro ECM setup. Chapter 4 describes the feasibility studies using the in-house built micro ECM setup. This is followed by the mathematical modeling of the anodic profile in the micro tool electrode fabrication process in Chapter 5. Details of the experimental work performed and results obtained in the ultra high aspect ratio micro tool fabrication process are described in Chapter 6. Subsequently, the conclusions are presented in Chapter 7.

CHAPTER 2

2. Literature Review

This section provides a detailed review of various literatures pertaining to this research. The overall review is divided into sections outlined as: (1) Electrolysis (2) Electrochemical Machining (3) Pulsed Micro ECM, (4) Bipolar Currents (5) Development of micro tools (6) Aspect Ratio of Microstructures and (7) Modeling of ECM

2.1. Electrolysis

Electrolysis is the basis of electrochemical machining. Electrolysis is defined as the chemical process that occurs when an electric current is passed between two conductors dipped into a liquid solution [24]. The liquid solution which contains the immersed conductors conducts electricity and thus completes the circuit. Such a liquid solution is known as an electrolyte. The conductors used in this case are called electrodes. One end connects to the positive end of the power supply and is called anode. The end connected to the negative end of the power supply is called cathode. The whole system of electrodes and electrolyte combined is known as an electrolytic cell. An ammeter attached in the circuit measures the flow of electric current in the circuit and gives a sign of the completeness of the circuit.

The electric current in an electrolyte is carried by atoms, better known as ions, which have lost or gained electrons, thus having a positive or negative charge [24]. Ions which carry a positive charge move through the electrolyte towards the cathode and are known as cations. Negatively charged ions travel towards the anode and are known as anions. These movements are a result of the applied potential difference from the power supply. This process can be used to remove material and also deposit material on the electrodes by making the metal ions move away or towards the electrodes. Electroplating is a popular application of electrolysis which involves metal coatings to be deposited on the surface of a cathodically polarized metal. Electropolishing is another popular application of electrolysis which is basically a material removal process from a metallic electrode [24].

Figure 3 shows a schematic of the electrolysis of iron in a sodium chloride solution. The prominent chemical reactions that take place in the electrolytic cell are described below [24].

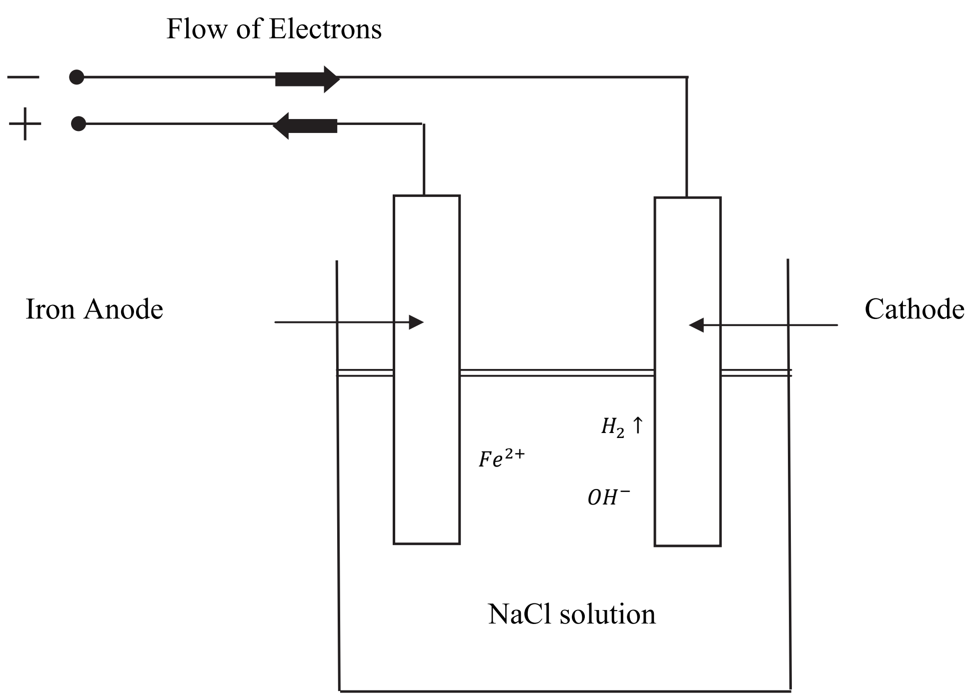

Figure 3 - Electrolysis of Iron

The anodic reactions are mainly the dissolution of iron into the metal ion. The breakdown of water results in oxygen being liberated [24].

$$Fe \rightarrow Fe^{2+} + 2e^-$$

$$H_2O \rightarrow 2H^+ + \ 2e^- + \frac{1}{2}O_2 \uparrow$$

The cathodic reactions are primarily the generation of hydrogen gas and hydroxyl ions [24].

$$NaCl \rightarrow Na^+ + \ Cl^-$$

$$H_2O \rightarrow H^+ + OH^-$$

$$2H^+ + 2e^- \rightarrow H_2 \uparrow$$

The overall reaction products are the formation of ferrous hydroxide due to the reaction of the metal ions with hydroxyl ions. Further reaction with water produces ferric hydroxide [24].

$$Fe + 2H_2O \rightarrow Fe(OH)_2 + 2H^+ + \ 2e^-$$

$$4Fe(OH)_2 + 2H_2O + O_2 \rightarrow 4Fe(OH)_3$$

Thus this overall electrolysis process shows the dissolution of iron from the anode and the generation of hydrogen at the cathode with some reactant products such as ferrous hydroxide precipitated out.

The amount of material change follows Faraday's two laws of electrolysis:

- The amount of material dissolved or deposited is proportional to the electricity passed
- The amount of material dissolved or deposited by the same quantity of electricity is proportional to their chemical equivalent weights.

These two laws are written as:

$$m = \frac{AIt}{zF}$$

Where,

m is the mass dissolved/deposited,	F is Faraday's constant
I is the current passed,	z is the valency,
t is the time,	A is the atomic weight,

2.2. Electrochemical Machining

Electrochemical machining (ECM) is a controlled anodic dissolution process of an anode and a cathode in an electrolytic cell during an electrolysis process [15]. In this process, the part to be machined is made the anode while the tool that does the machining is made the cathode. The anodic dissolution rate which is the rate at which the anodic metal is removed depends on the electrochemical properties of the metal and the current passed [24]. The cathode or the tool remains unaltered by the electrochemical machining process which gives ECM an edge over many other processes, as there is no tool wear or any other need to change the tool. Machining the anode usually involves giving it simple or intricate shapes. For this purpose, the tool electrode used can either be simple or complex shaped. A complex shaped tool electrode is typically sunk vertically downward during the machining process and the anode takes the shape defined by the cathode or the tool electrode as shown in the top part of figure 4. In a simple shaped tool which moves in a designed path to achieve the final required shape of the anode, the output is not dependent on the shape of the tool but on the path undertaken by the tool. This is shown in the bottom part of figure 4. This is usually used in deep hole drilling and other applications such as electrochemical turning, milling, polishing, etc [25].

The term micro-machining refers to material removal of small dimension ranging from 1 – 999 μm [16]. The fabrication of micro sized features or parts using ECM is known as micro electrochemical machining (micro ECM). There is a large application of micro ECM in the semiconductor, biomedical, automobile, cosmetic and painting industries. It primarily involves the use of micro sized tools with small inter-electrode gaps of the order of 5 – 50 μm in the presence of a pulsed power supply and the use of a pumping electrolyte solution to flush out the reactant products possible [16, 26, 27]. A recent advancement is the use of a pulsed power supply with emphasis on short pulses for the micro ECM process [16]. Effects of maintaining a really small inter-electrode gap and monitoring it on-line has also been explored [17]. Some of the research work done in the past has been reviewed in the subsequent sections.

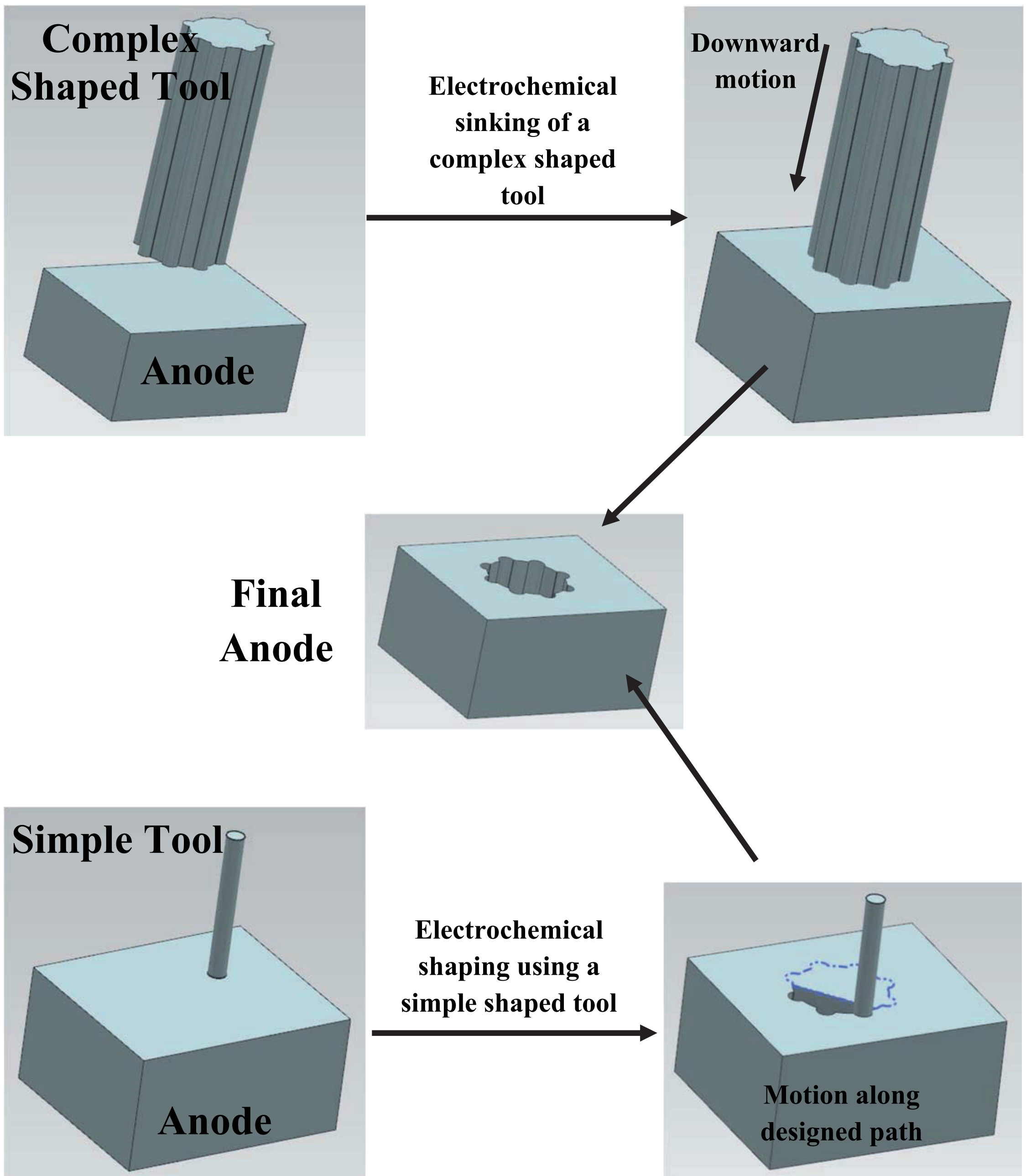

Figure 4 - Electrochemical shaping

2.2.1. Advantages and Applications of Electrochemical Machining

Electrochemical machining is known for its several advantages and thus has been widely used in various applications. Some of the popular advantages of ECM are listed below [7].

a) Independent of the hardness of the anode material

b) No tool wear. Being a non-contact process, it is free from deformation, breakage etc.

c) High material removal rate.

d) Free of thermal stresses.

e) Burr free machining

f) Easy to machine complex features

g) Ability to machine a wide range of conductive materials

The most popular applications of electrochemical machining have been listed below and illustrated with figures 4 -9.

a) Deburring (Figure 5)

b) Electrochemical shaping (Figure 4)

c) Hole drilling (Figure 6)

d) Electrochemical milling (Figure 7)

e) Electrochemical turning (Figure 8)

f) Electrochemical polishing (Figure 9)

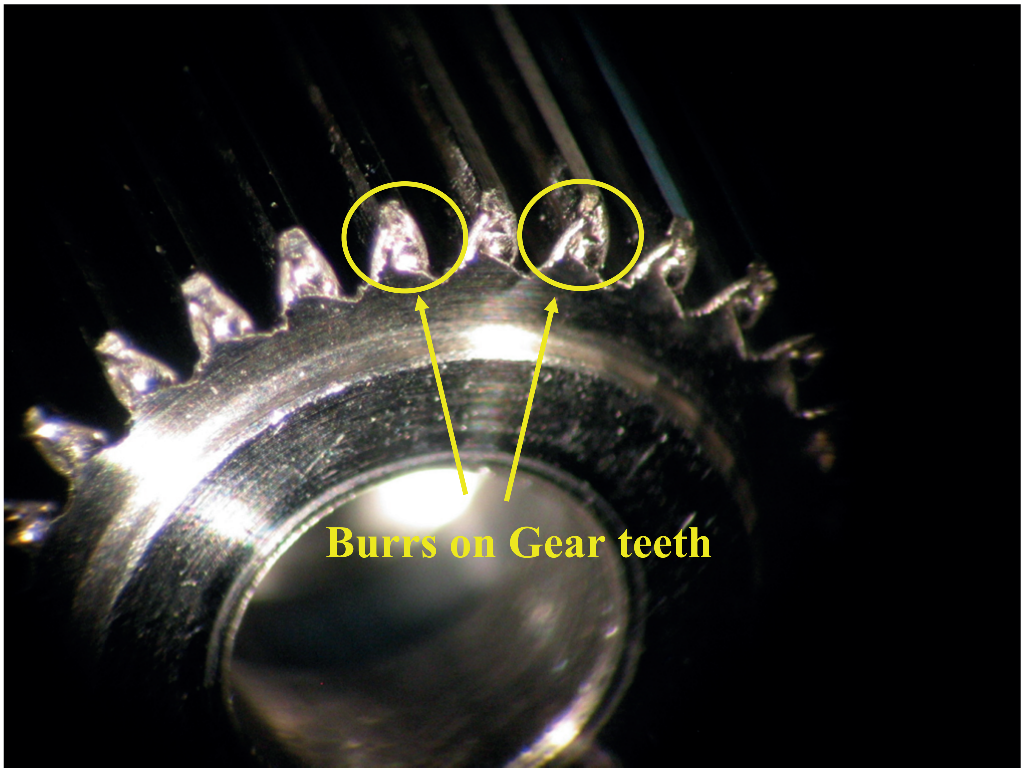

(a)

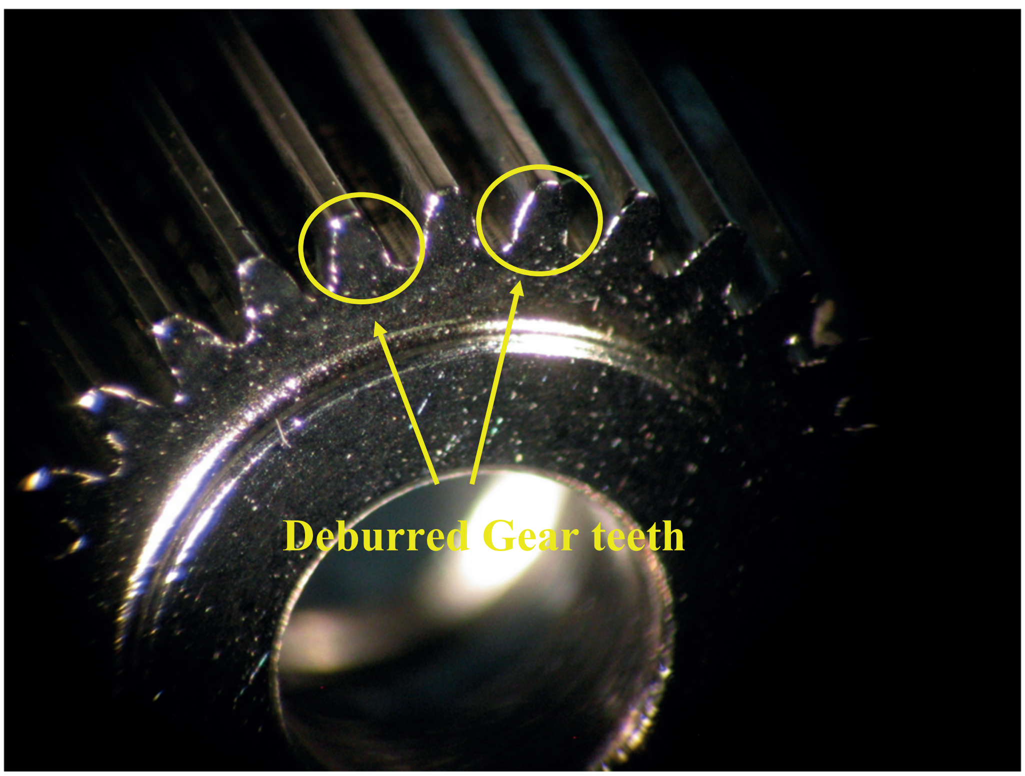

(b)

Figure 5 - Electrochemical Deburring on Gears [28]

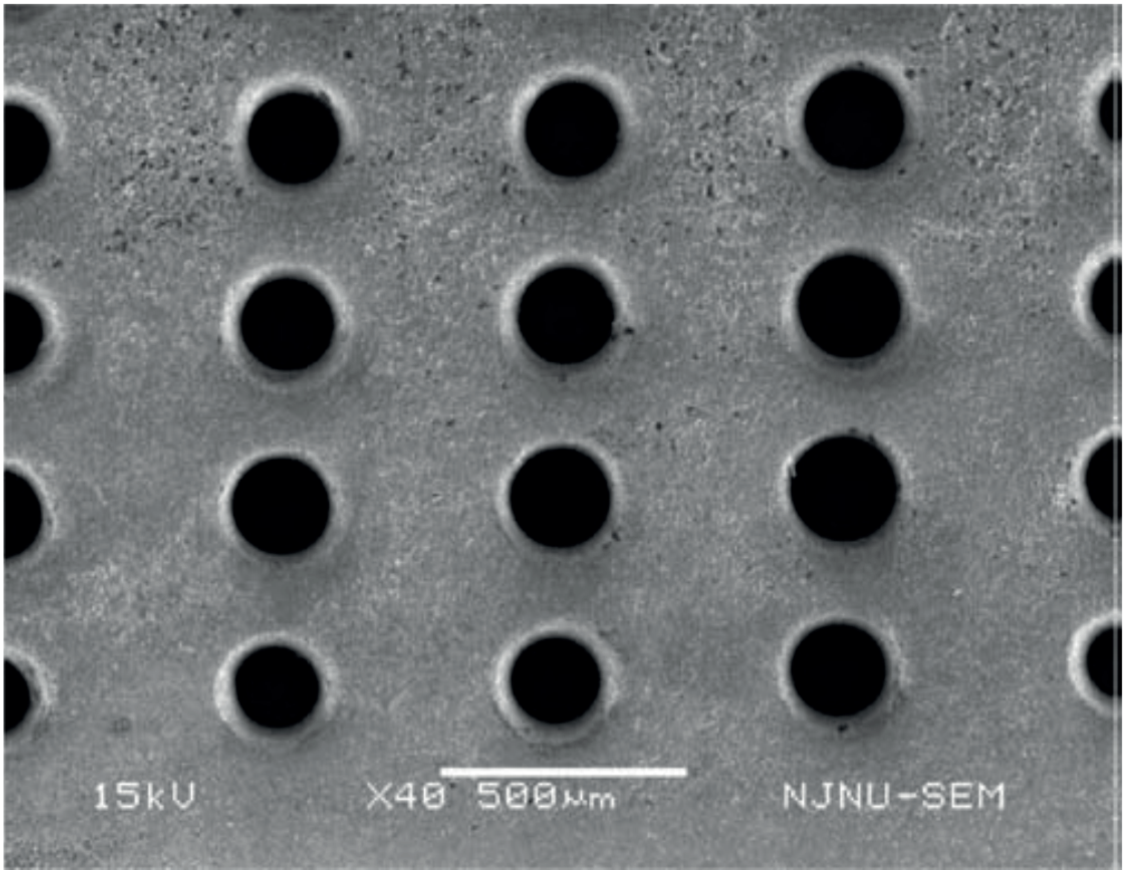

Figure 6 - Stainless Steel plate 100µm thickness: Multiple micro-holes machined by micro-ECM, Voltage = 5V, Feed rate = 100µm/min, Pulse on time = 30 µs, 0.5% electrolyte concentration [29]

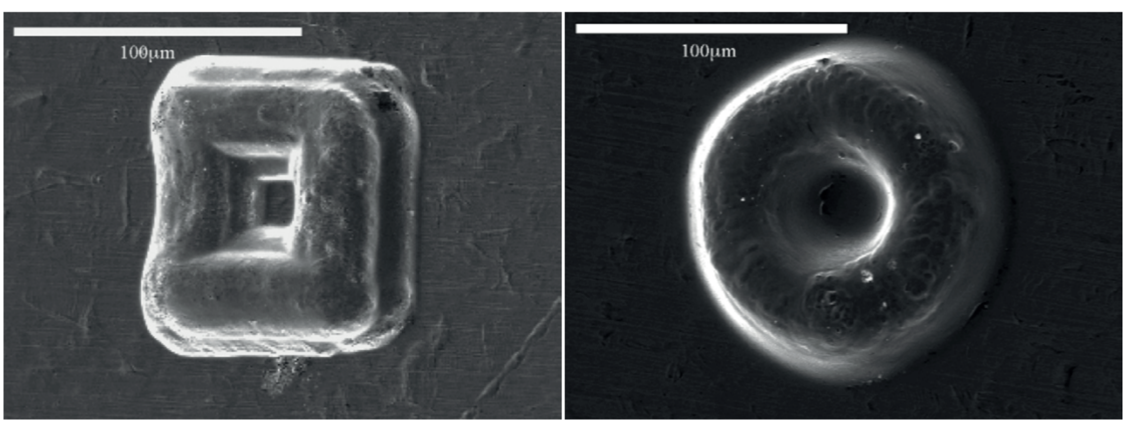

Figure 7 - Stainless steel plate: Micro Square and circular cavity with central island, 250 ns pulse duration, 1MHz, 7V pulse amplitude [30]

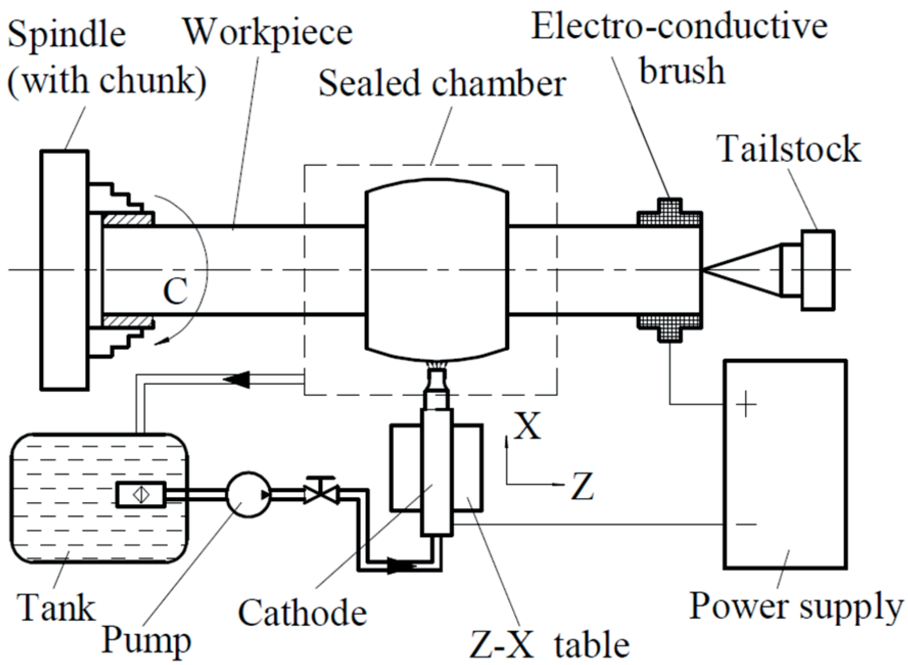

Figure 8 - Schematic illustration of Electrochemical Turning [31]

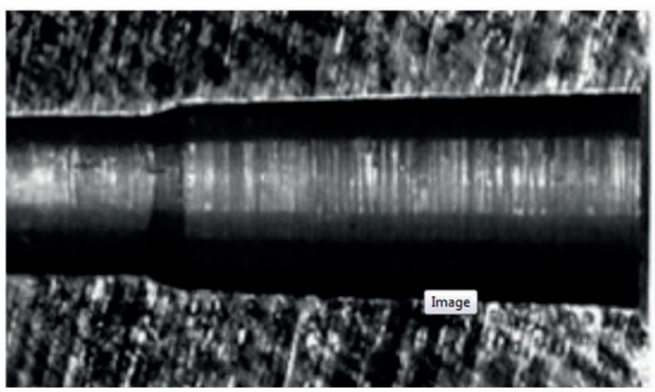

(a)

(b)

Figure 9 - Electrochemical polishing on sample: (a) before and (b) after [32]

2.3. Pulsed Micro ECM

An important aspect in the successful use of micro electrochemical machining is the use of a pulsed power supply. A pulsed current can be defined as a high instantaneous current density followed by an off time during which no current flows [33]. This set of pulses is repeated with various magnitudes of on and off pulses depending on the requirement. Figure 10 shows a representation of the pulsed current at 0.25A and an equal forward and reverse pulse on-time of 5 ms and a pulse off-time of 5 ms. Application of pulsed voltage is required to avoid problems of non uniform dissolution of work piece and temperature rise [26]. The use of pulsed current also enables the recovery of gap during the pulse off-time thus giving improved dissolution and accuracy and surface finish as compared to continuous current [16]. Micro ECM relatively requires a low current density in the range of 75 – 100 A/cm^2 and a voltage of about 4-10 V [16, 26].

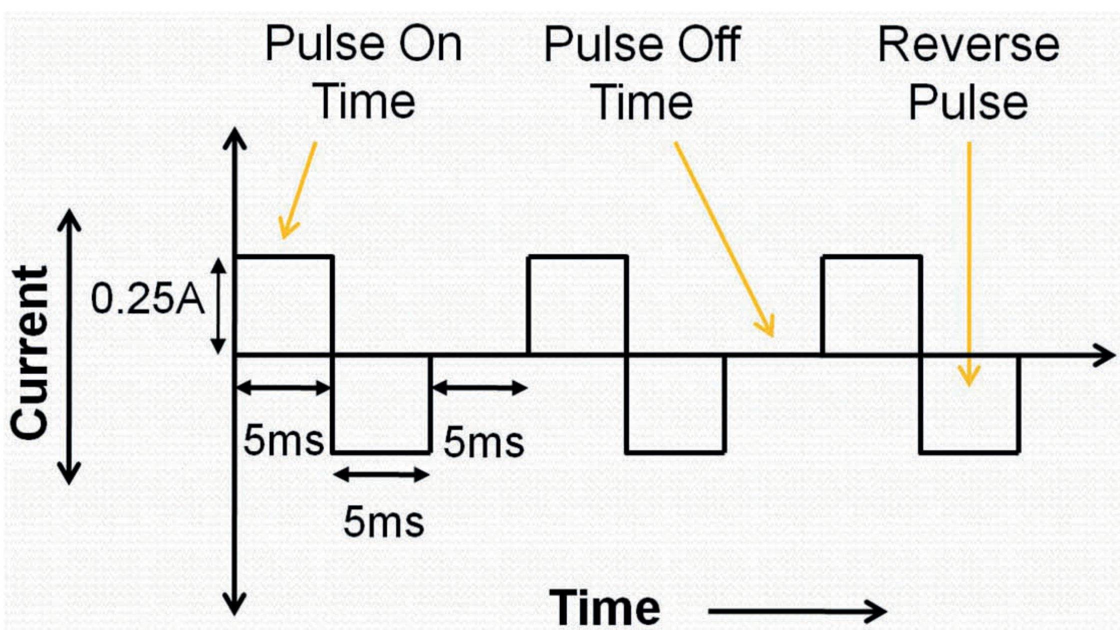

Figure 10 - Representation of Pulsed current with time

A pulsed power supply is used for micro ECM for making a triangular shaped microcavity slot of width 160 μm and a pentagonal microcavity of 180 μm as shown in figures 11 and 12 respectively using 5V pulses of 1 MHz frequency with an inter electrode gap of 20 μm and a tool electrode feed of 20mm/min [27]. Application of short pulse voltages assists the machining to be stable at small gaps [15]. Micro holes of 20 μm depth were machined using a 35 μm diameter insulated electrode by varying the pulse on-times from 30 ns to 160 ns and keeping a constant feed of 0.1 μm/s and a fixed pulse period of 1 μs [34]. Figure 13 shows the SEM images of the various micro holes machined and figure 14 shows the variation of the diameter and gap according to the pulse on-time [34]. The inter-electrode gap or the machining gap is very important parameter in micro ECM. A low inter-electrode gap helps in increasing the local dissolution process [15]. Use of smaller inter-electrode gaps tends to provide a better machining accuracy [16, 26, 35]. Factors influencing the inter-electrode gap have been shown mathematically [35]. It was reported that lower voltage, lower electrolytic concentration, higher rate of rotation of the tool, higher feed rate of the tool and a shorter pulse time result in decreasing the inter-electrode gap and thus increasing machining and shape accuracy. The significance of maintaining the inter-electrode gap at the range of 15-20 μm consistently to achieve high accuracy and surface finish was mentioned [16]. 10 μm deep holes were drilled with a tool electrode of diameter 60 μm to investigate the effects of machining gap on electrolyte concentration, pulse on-time, pulse voltage and machining time [36]. The findings indicated the machining gap to increase with electrolyte concentration, pulsed voltage, pulse on-time and machining time. An electrical conduction method to control the inter-electrode gap has been described in [26]. Electrical contact can be determined by checking for current on supplying 1 V between the electrode and the work piece. If there is contact, the tool is fed upwards in steps until the contact is broken. This is then used to control the feeding and positioning of the electrode and hence the inter-electrode gap. A similar inter-electrode gap control system for micro hole drilling is discussed in [17]. After the tool electrode is placed at an initial gap from the anode, the tool is fed towards the anode and the machining current is sampled. When there is a sharp current jump, the system shows a short circuit and the tool electrode is withdrawn to maintain the small gap. An ultrasonic measurement system for a dynamic inter-electrode gap using its relationship with time was also formed [6]. It was successfully found to apply the use of ultrasound as a passive, non-intrusive, in-line gap measurement system for ECM.

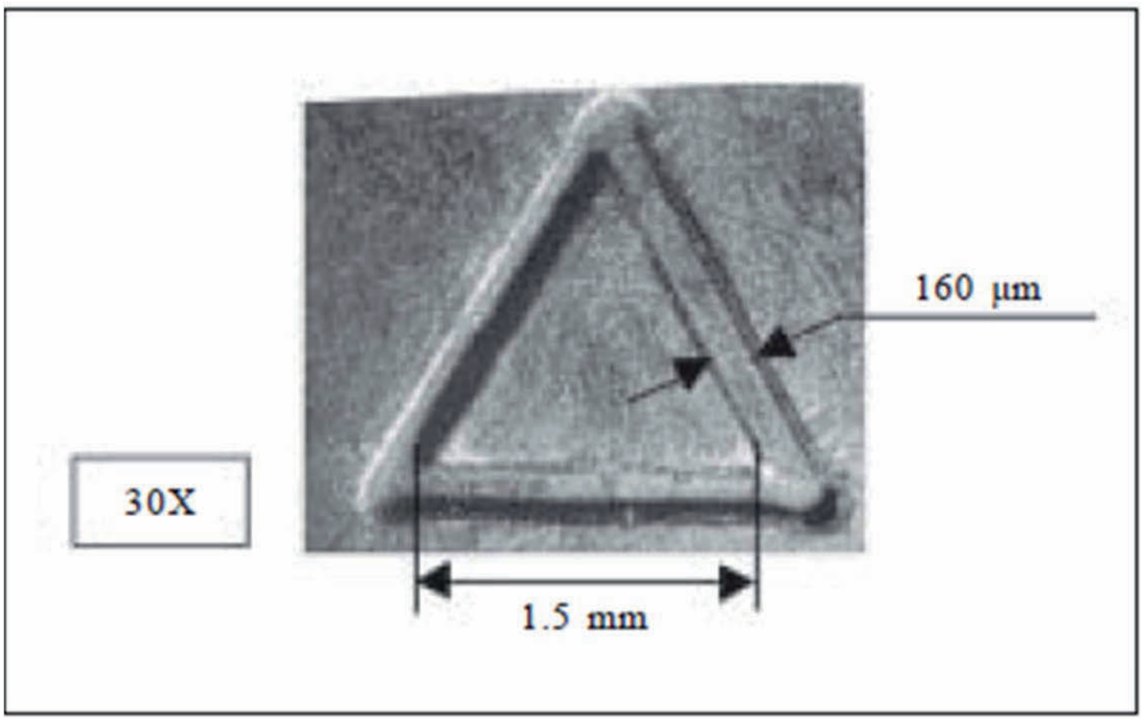

Figure 11 - Triangular Microcavity by micro electrochemical machining [27]

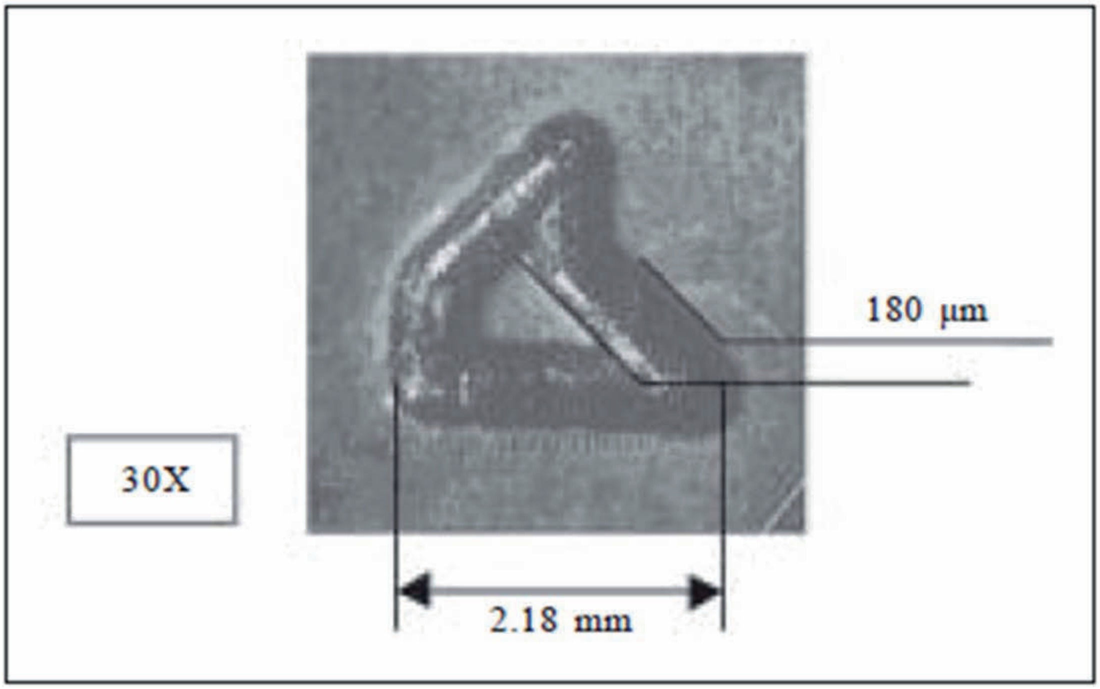

Figure 12 - Pentagonal Microcavity by micro electrochemical machining [27]

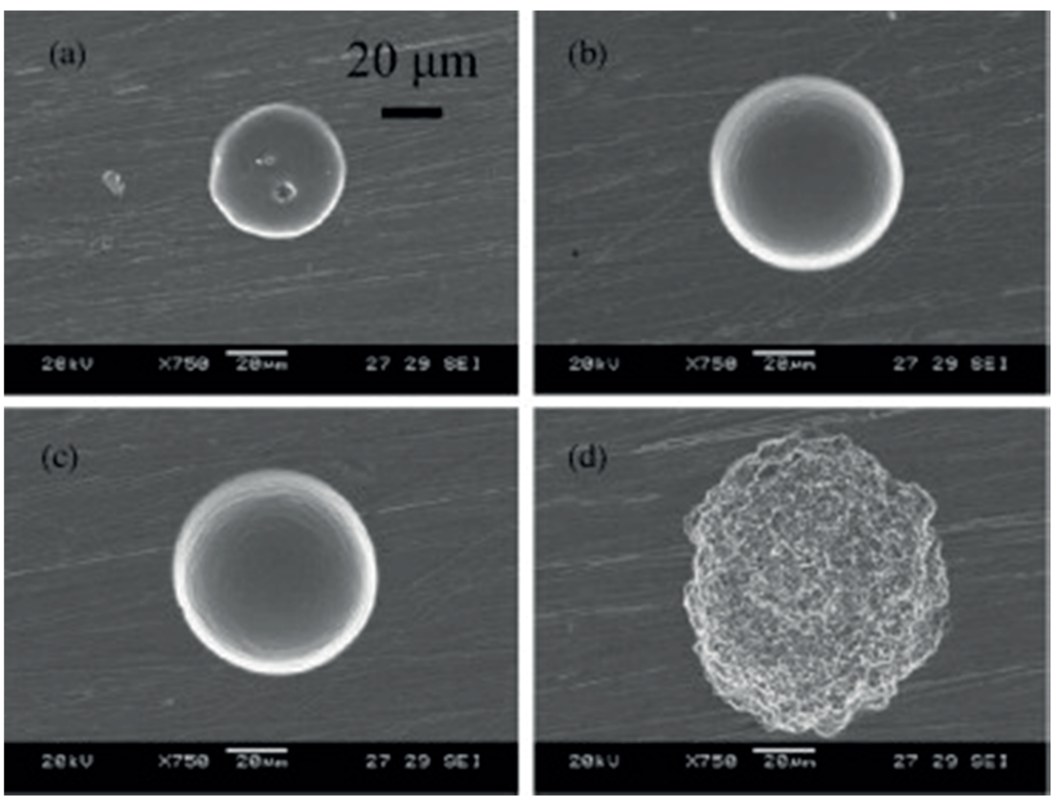

Figure 13 - SEM images of micro holes according to pulse duration: (a) 30 ns, (b) 90 ns, (c) 120 ns, (d) 160 ns [34]

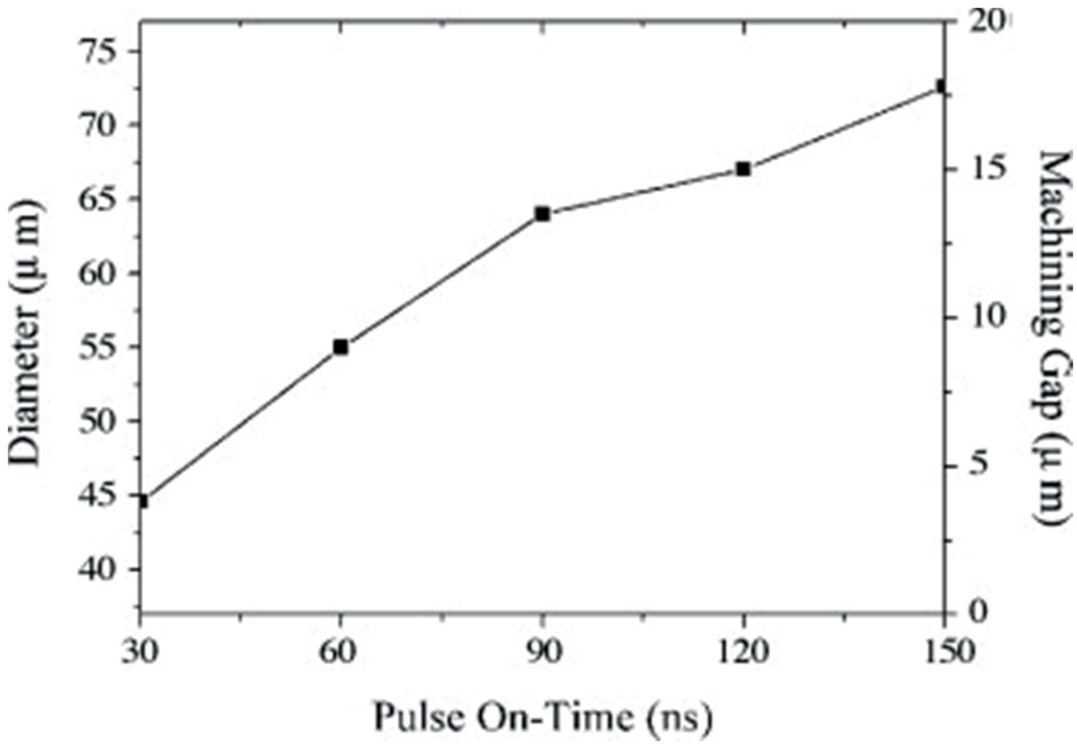

Figure 14 - Diameter and machining gap according to pulse duration [34]

The inter-electrode gap is also an important concept for the material removal in micro-machining [26]. It is required to improve the machining rate and accuracy to achieve the full potential of electrochemical micromachining [18]. Some research was done in micro ECM using a response surface methodology based approach to find relationships between various micromachining process parameters and the material removal rate [37]. A mathematical model was developed to represent the relationship between MRR and the controlling variables such as voltage pulse on/off ratio, machining voltage, electrolyte concentration and voltage frequency. Material removal rate was found to increase with an increase in machining voltage at all electrolyte concentrations; however at a very low inter-electrode gap, the MRR did not increase linearly with the machining voltage [18, 37]. Increase in electrolyte concentrations resulted in a linear increase in MRR as larger number of ions are involved with the process resulting in more machining [18, 37]. MRR increases initially with increase in pulse on/off ratio as there is more machining time, however as the on/off ratio increases further, it results in a very little off time, thus not allowing the reaction products to be removed properly and hence resulting in an improper dissolution of the anode and reduction in MRR [37]. The variation of material removal rate (MRR) with the machining voltage, the electrolyte concentration and the pulse on time is shown in figure 15 (a), (b) and (c) respectively [18].

2.4. Bipolar Currents

Several passive metals and alloys tend to form an insoluble passive oxide film in neutral electrolytic solutions which prevents further dissolution of anode [38-40]. A bipolar current is essentially the application of a forward (anodic) pulse followed by a reverse (cathodic) pulse and a relaxation period [40]. It was found that during the reverse pulse period, the nascent hydrogen and oxygen could be consumed in the reaction which disables metal hydroxide precipitation on the tool and reduces the oxide film formation [40]. This helps maintain the tool size and shape and prevents surface defects [40]. Forward and reverse pulses of 0.5 ms were used for the electrochemical finishing of tungsten carbide in sodium nitrate ($NaNO_3$) with a electrode gap distance of 50 μm under a current density of 100 A/cm^2 to obtain a removal rate of 0.17 μm/(C/cm^2) thus successfully demonstrating the electrochemical dissolution of tungsten carbide alloy with a bipolar pulse train [39].

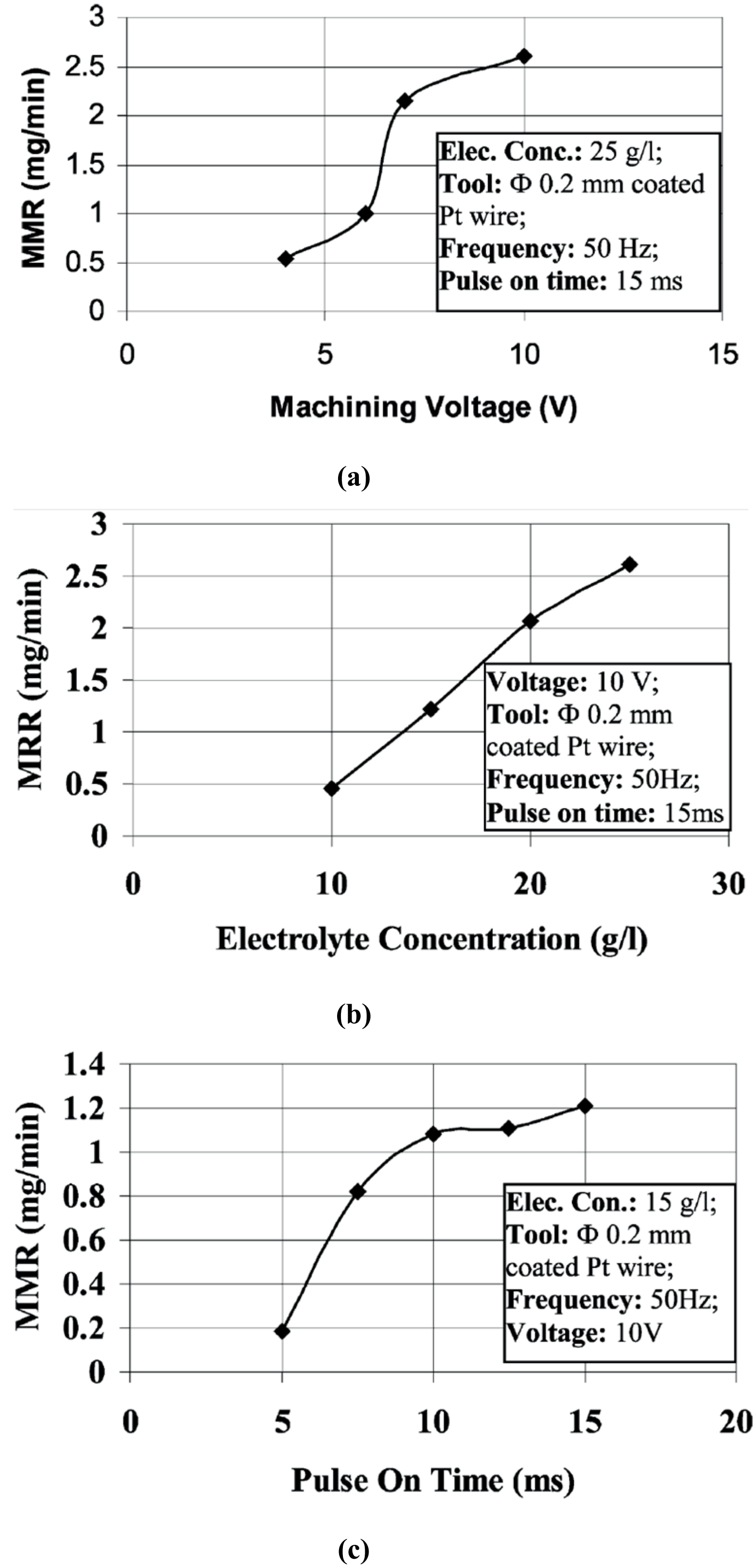

Figure 15 - Variation of MRR with (a)machining voltage, (b)electrolyte concentration, (c)pulse on time [18]

2.5. Fabrication of Micro Tools

In order to achieve a high machining accuracy, it is essential that the micro tool itself is of high accuracy and precision. Micro tools are mainly fabricated using processes such as electrochemical etching and wire electro-discharge grinding (WEDG), micro electro-discharge machining (μEDM) [9, 15, 17, 41]. An on-machine method for fabricating high aspect ratio micro structures using EDM has been described in [42]. It was claimed that clamping the tool electrode just once in the whole process avoids clamping errors and greatly increases machining precision. Figure 16 (a) describes the on-machine fabrication of tool electrode using a sacrificial electrode which can also be placed in multiple configurations [42]. Figure 16 (b) describes an on-machine measurement of the tool electrode diameter using an optical measurement device [42]. The tool electrode is machined till it reaches the required diameter then it is used to machine high aspect ratio micro structures as shown in figure 16 (c) [42]. This process enables both micro tool fabrication and machining using EDM on the same base and result in high precision output.

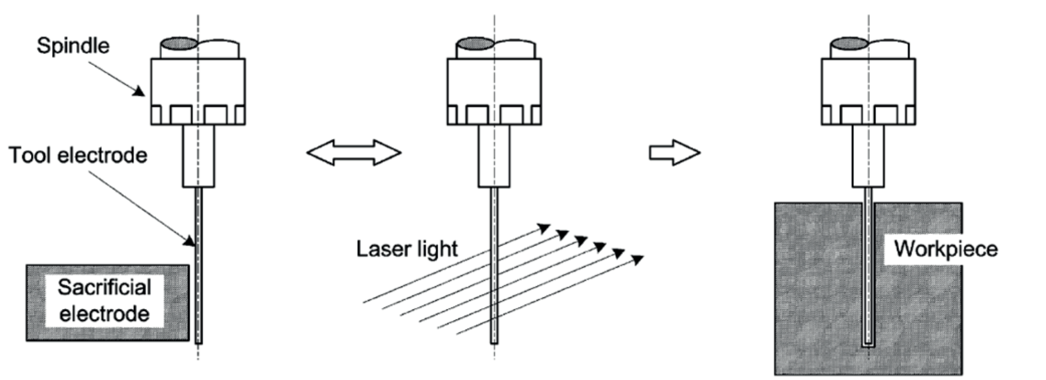

(a) On machine tool electrode fabrication by micro EDM   (b) On machine optical measurement   (c) Fabrication of high aspect ratio micro structure by EDM

Figure 16 - On-machine process to fabricate high-aspect ratio micro-structures using micro-EDM [42]

A tapered tungsten microelectrode with a diameter of 7 μm was obtained by micro ECM using a machining voltage of 10 V, electrolyte concentration of 40% and a pulse on-time of 50 μs with a power supply of 10kHz [43]. Figure 17 (a) shows the tungsten micro electrode fabricated by micro ECM [43]. The tip of the micro-electrode is shown in figure 17 (b) and the radius of the tip is found to be 50 nm [43].

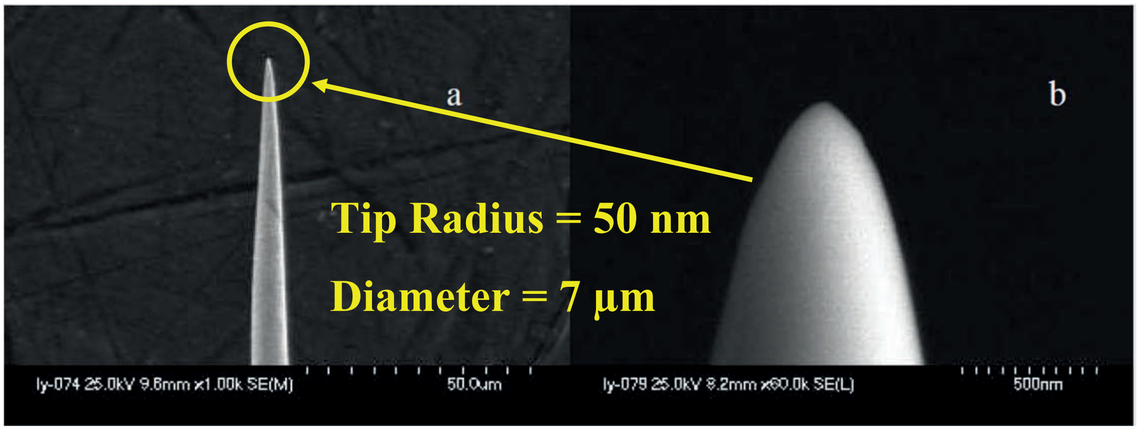

Figure 17 - Tungsten microelectrode fabricated by micro ECM [43]

The effect of some of the process control parameters such as current density and machining voltage on the final shape of the microelectrode in a micro ECM process has been described in [44]. It was explained about the influence of current density on the diffusion and movement of ions and the formation of a diffusion layer when the anodic dissolution rate is higher than the ionic diffusion rate, which prevents ions going from the anode to the electrolyte. A conical shaped tool is obtained under low current density and voltage conditions as the dissolution of the anode is lesser than the ion diffusion rate as shown in figure 18 (a) [44]. A higher current density and voltage result in a reverse conical shaped tool due to the anodic dissolution rate being higher than the ionic diffusion rate and the diffusion layer particles moving along the tool surface downwards due to gravity as shown in figure 18

(c) [44]. The application of the appropriate amount of current density and machining voltage results in cylindrical shape of the microelectrode as shown in figure 18 (b) [44].

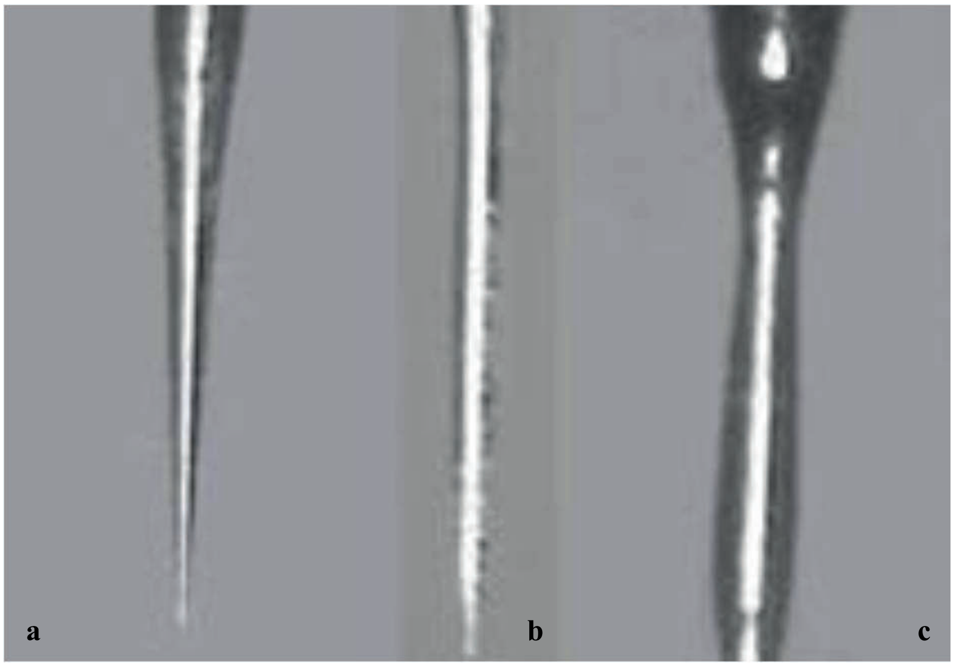

Figure 18 - Effect of current density & machining voltage on shape of microelectrodes machined in ECM [44]

A relationship between the applied electric charge, and the etched tool electrode was defined by the initial diameter, final diameter including terms of the immersion depth, extended submerged length due to surface tension and other electrochemical constants [45]. A similar representation was used to study the effects of various parameters such as voltage, pulse period, duty cycle, and electrolyte temperature during the fabrication of a tungsten tool electrode [46].

2.6. Aspect ratio of micro structures

There is a growing industrial need to produce high aspect ratio micro tools to fabricate small and deep micro holes [47]. It was suggested to use longer thin tool electrodes fabricated from micro EDM process to make high aspect ratio micro features [42]. High aspect ratio tool electrodes with tungsten and tungsten carbide materials were fabricated using WEDG process achieving aspect ratios of 150 and 250 respectively [48]. However, making high aspect ratio micro tool by micro ECM has not yet been adequately studied. Figure 19 shows a thin and long micro rod produced by deep immersion method using electrochemical etching with a diameter of 30 μm with an aspect ratio of 100 [49]. Micro tools with aspect ratios ranging from 20 to 50 were developed using micro ECM [50]. A micro electrode of molybdenum was fabricated with a diameter of 12 μm and a length of 1 mm giving an aspect ratio of about 83 [51]. It was fabricated with 1 μs pulses of 3V voltage in 2M NaOH and it is shown in figure 20 [51].

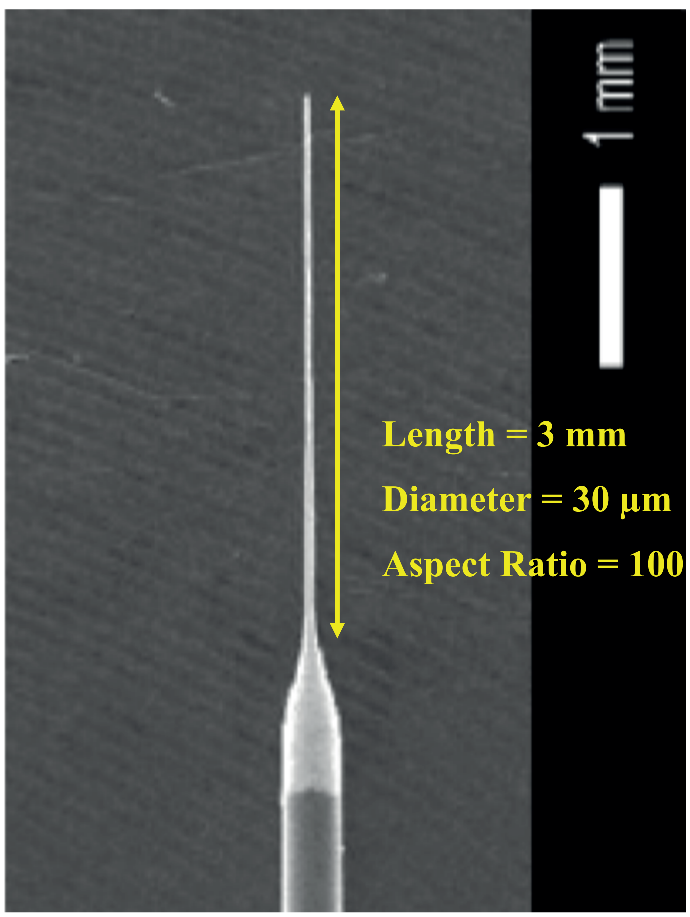

Figure 19 - Micro rod of 30 μm diameter made by ECM [49]

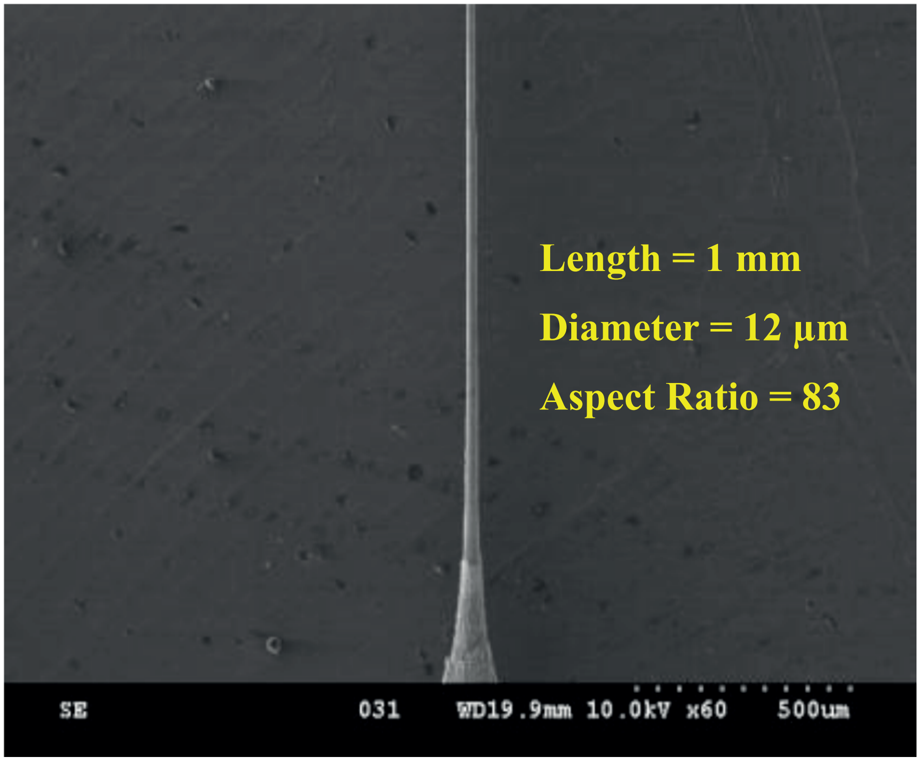

(a)

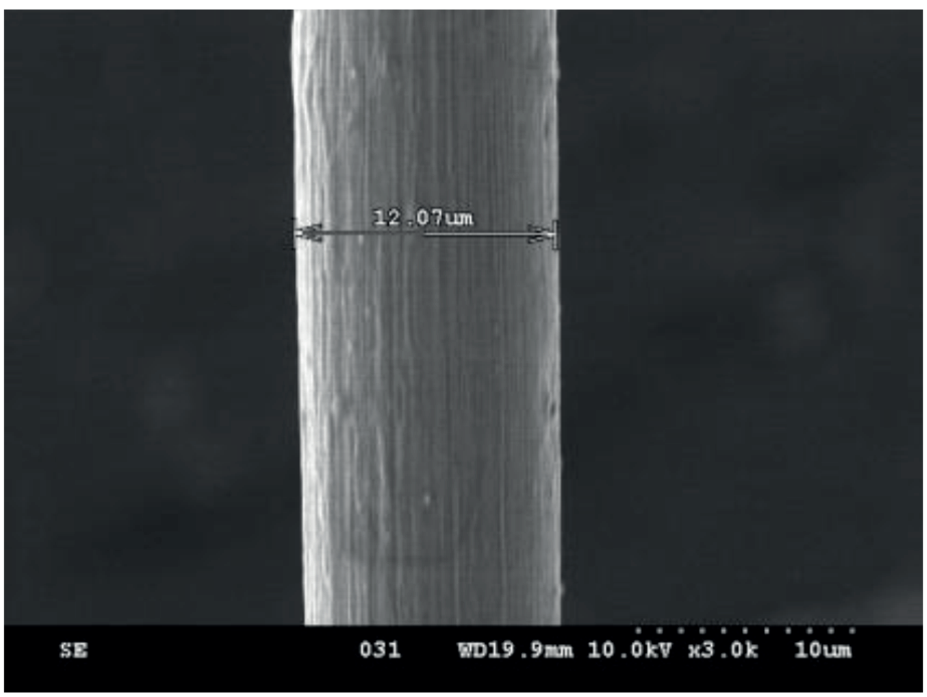

(b)

Figure 20 - Molybdenum electrode of a 12 µm diameter and 1 mm length. (a) Tool Electrode (b) Local area showing 12 µm [51]

Table 1 shows the aspect ratios of some of the high aspect ratio tools developed by various processes.

Table 1 - Literature review of high aspect ratio micro tools

Material	Diameter	Aspect Ratio	Method	Reference
Brass	60 µm	33	EDM	[52]
Tungsten	40 µm	75	EDM	[47]
Tungsten	20 µm	150	WEDG	[48]
Tungsten Carbide	20 µm	250	WEDG	[48]
Molybdenum	12 µm	83	Micro ECM	[51]
Tungsten Carbide	30 µm	100	Micro ECM	[49]

2.7. Modeling of ECM

Mathematical models have been developed for electrochemical machining, to determine the interelectrode gap or the surface potential or other parameters. A model to determine the minimum interelectrode gap limited by the electrolyte boiling for a pulse electrochemical machining process was developed in [53]. It was concluded that a shorter pulse on-time resulted in smaller gaps. Another mathematical model of a shaping process by a numerically controlled ECM with a ball end tool electrode was developed in [54]. Using a finite difference method, a software was developed to simulate the anode shape evolution. Figure 21 shows an example of the results of the simulation of ECM shaping [55]. The top portion has a constant feed while the bottom half has an additional oscillating motion of the tool electrode. The theoretical predictions seem to agree with the experimental results.

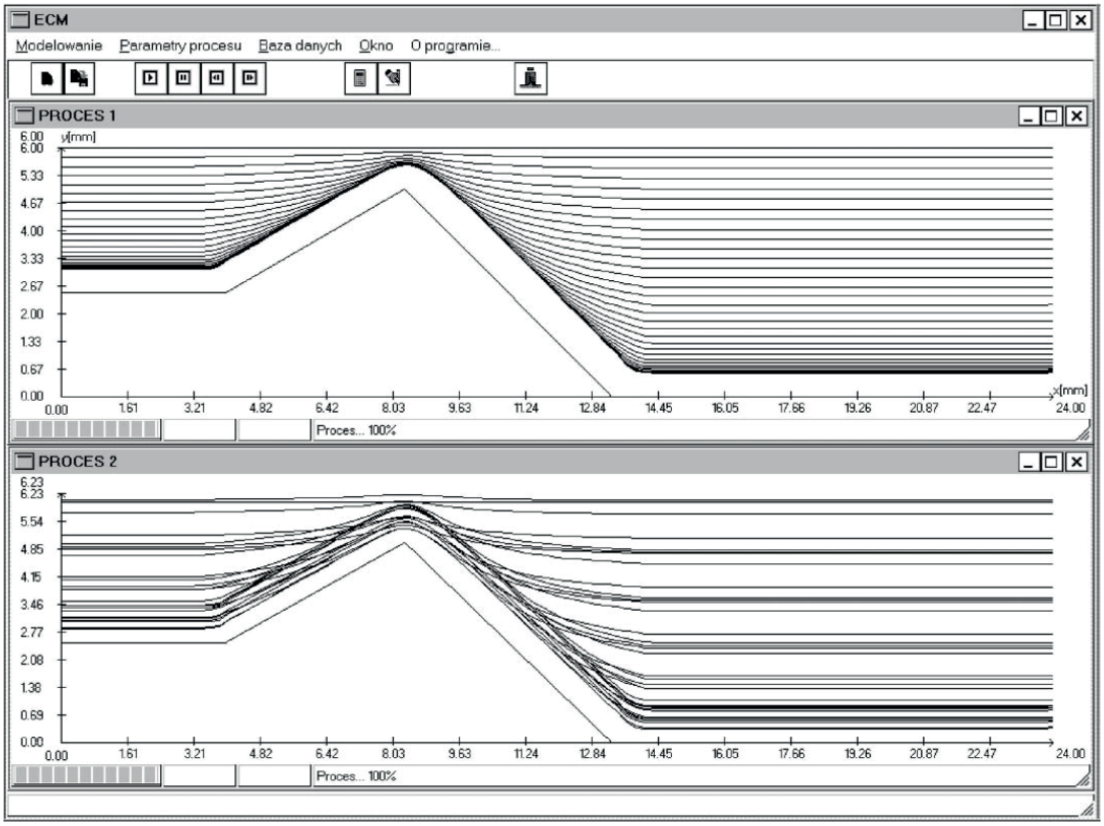

Figure 21 - Example of simulation of ECM-CNC shaping process [55]

Using a standard Boundary Element Method and a ‘marker method’, a model for the 3D simulation of electrode changes during an electrochemical machining process was developed [56]. A simulation for ECM process of the letter ‘E’ shaped cathode moving towards the anode at a speed of 0.1 mm/s was performed for a total ECM time of 34 minutes divided in 10 time steps. The interelectrode gap between the anode and the cathode was taken to be 0.2 mm, and the potential applied between the electrodes was 10 V. The electrolyte taken was $NaNO_3$ solution of a 70 gm/l concentration and at a temperature of 27 °C. Figure 22 shows the triangular meshed image of the configuration of the ECM system with the ‘E’ shaped cathode moving down towards the anode [56]. Figure 23 (a) shows the current density distribution at the last time step and (b) shows the final anode profile obtained [56].

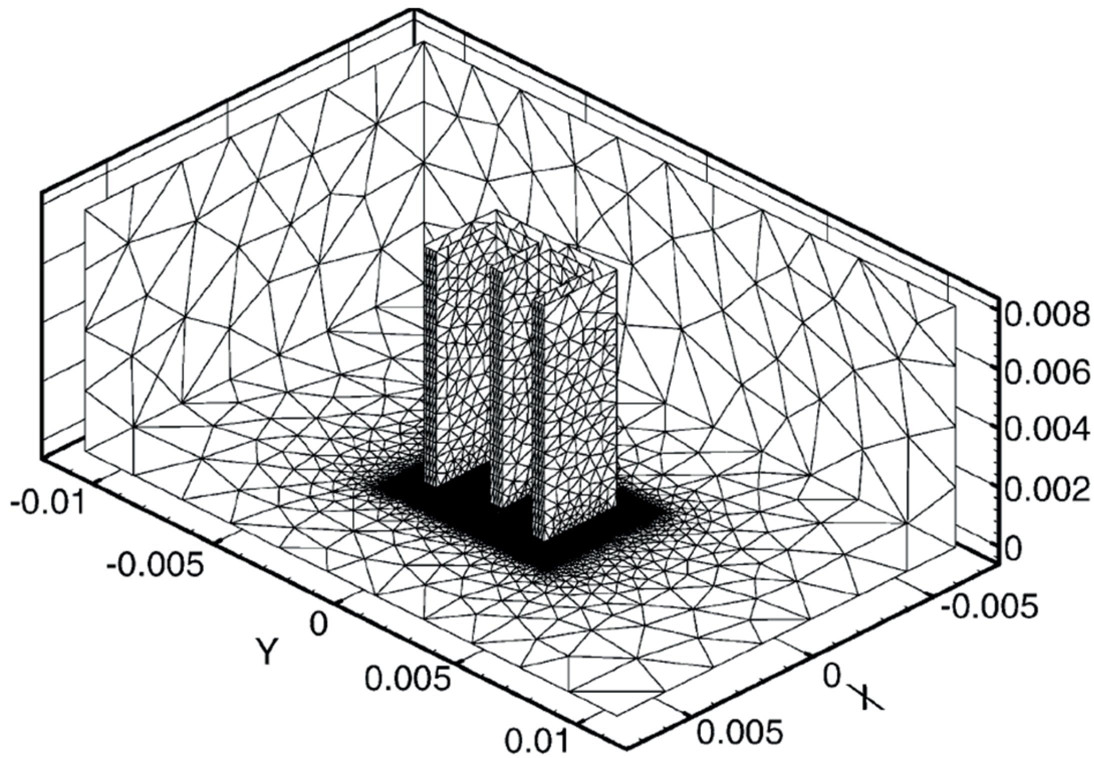

Figure 22 - ECM system configuration and triangular mesh [56]

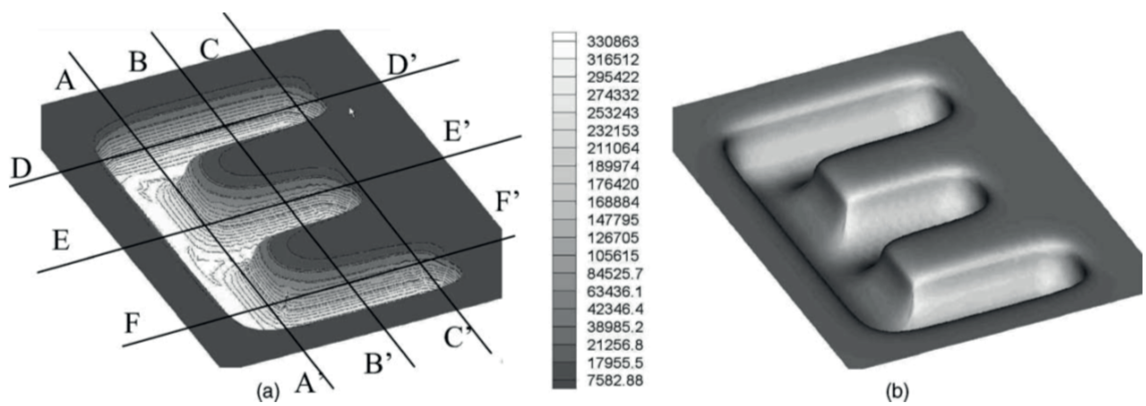

Figure 23 - (a) Current distribution at the last time step. (b) Final anode profile (A/m^2) [56]

A mathematical model and a software were developed to simulate the electrochemical machining of complex 3D microstructures of high accuracy using ultrashort pulses [57]. The developed model is useful for pulse electrochemical micromachining (PECMM) process analysis, surface shape prediction and optimization. Another mathematical model was developed to analyze the anodic smoothing characteristics in a pulse electrochemical finishing (PECF) process [58]. Factors such as the finishing time, the interelectrode gap, the applied voltage and the rotational speed of the electrode were explained through the model and using this, parametric studies on the pulse electrochemical finishing process were conducted. The model was adapted from the basic anodic recession rate and formulated as [58]:

$$ds = \frac{\eta \kappa_e k_v (U_0 - \Delta U)}{S} dt$$

This model was further developed to explain the mechanism of anodic smoothing of a real surface and successfully predicted the experimental results.

Based on the above literature review, a pulsed micro ECM system is developed in-house to fabricate high aspect ratio micro tools as described in subsequent chapters. As the literature suggested, short pulsed voltage has been used, low current density is used and a very small gap is maintained between the electrodes. Also, reverse currents are used to machine passive materials. A mathematical model has been developed to predict the diameter of the tool electrode (anode) based on the velocity of the cathode movement.

CHAPTER 3

3. System Design

This section describes the various system components used in the in-house built micro ECM setup. It explains the various design considerations and capabilities of the various components.

3.1. Introduction

The in-house built micro ECM setup was made out of several components. The schematic of the whole setup is as shown in figure 24.

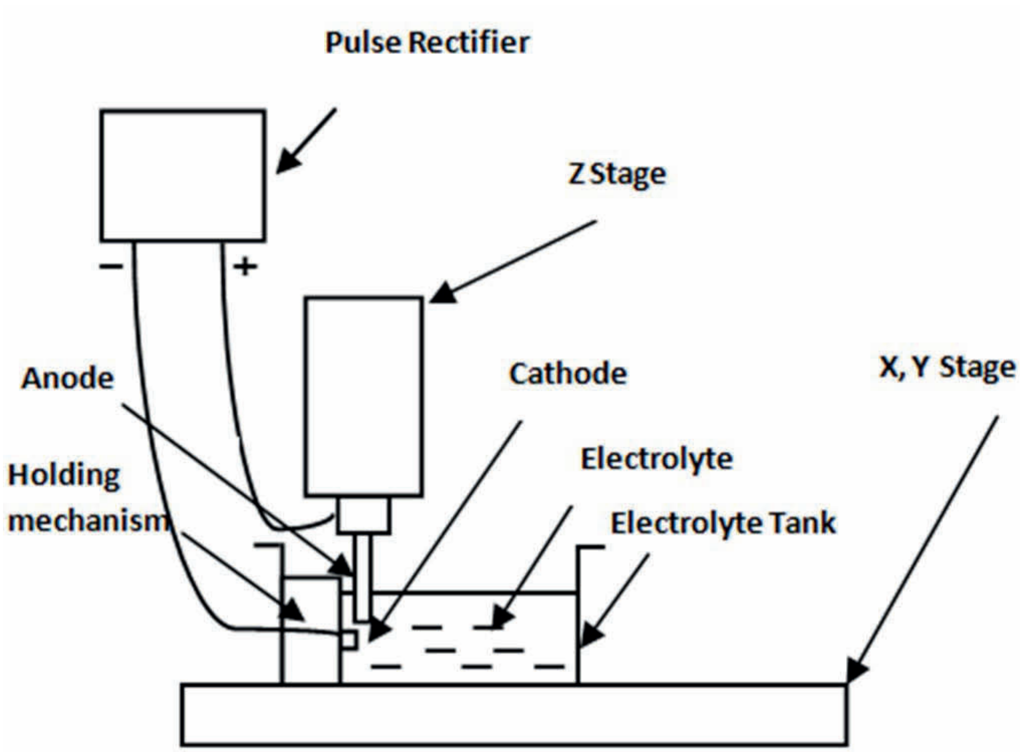

Figure 24 - Schematic of the Micro ECM setup

The various components of the setup are listed below:

i. XYZ-LSMA System & ST3 controller

ii. DμP(R) series W/Microstar pulse power supply

iii. DM 2400 CNC milling machine (used as a platform)

iv. Anode

v. Cathode

vi. Electrolyte

vii. Tool Positioning method

3.2. Design Considerations

A number of design considerations were taken into account in order to produce an effective and accurate means of machining. Some of the design considerations are mentioned below.

3.2.1. High accuracy and precision

Being a micromachining process, it is imperative that the whole system is as accurate and precise as possible. The XYZ stage is required to be highly accurate and precise in its measurement. Especially as it governs motion in all three axes, it is crucial that the stepper motor accurately moves the stage. It is important for the tool positioning method to be as accurate as possible with a low repeatability due to the low gap between the anode and the cathode.

3.2.2. Suitable Materials

Choosing the right materials for the process is a defining step for the research involved. Several properties of the anode, cathode, electrolyte, electrolytic tank have to be taken into account while choosing the materials. Using knowledge about these from literature is an essential step. Other considerations include the effects of each of these materials individually and upon reaction with each other. Corrosion is one such important factor to look into as the electrolyte solutions have a tendency to corrode the metal electrodes or the electrolytic tanks that come in contact with them for extended periods of time. The materials chosen should be as corrosion resistant as possible. It is also necessary that all the materials used are environmentally friendly and can be disposed safely. Especially with the use of acids, it could lead to disposal problems. Materials chosen for the anode should also be considered based on the application of the anode from a research and an industrial perspective.

3.2.3. Preventing unwanted machining and losses

Since the anode and the cathode are connected to the power supply via metallic wires, there are lots of unwanted machining areas within the electrolytic system and outside. In order to prevent any chance of machining from these areas it is important to insulate all the areas within the electrolytic system except the required anodic and cathodic areas. Lack of insulation in those unwanted areas can lead to unwanted and ineffective machining and undesired results in the final product. It is also important to ensure the wires are insulated as much as possible on the outside to prevent the overall power losses to the system.

3.3. XYZ-LSMA System & ST3 controller

The integrated multi-axes XYZ systems built with LSMA-184 Series motorized actuators shown in figure 25 provide travel up to 13 mm in each axis. They are driven by a Stepnet ST3 stepper motor driver which combines three stepper motor drivers in one package and gives a complete digital control. The stages are built with a precision bearing system and these motorized stages offer a high-resolution up to 0.15 micrometers. The actuator has a low profile high-stability compact and monolithic design as its main feature and together with its high resolution it makes the device ideal for its integration in high precision measurement and manufacturing systems. A compact and light-weight stage in itself, it can carry a load up to 3kg in the vertical axis and 10 kg in the horizontal axis.

The major advantages of using this XYZ-LSMA system are [59]:

- Simplicity of the design allows the linear actuators to produce direct motion, eliminating stretching belts, slipping pulleys and wear of lead screws
- These contain built in bearing systems which require no adjustment or maintenance requirements or the use of any lubricants.
- They ensure a high repeatability of 0.0001" and displacement accuracy of 0.0005" without the expense of feedback devices.
- The system is highly flexible and can be easily rearranged to provide alternate configurations covering motions in all planes.

Figure 25 shows an image of the XYZ-LSMA 184 stage which comprises of three linear actuating stages. The use of such an accurate positioning system is crucial for effective machining in a highly controlled manner.

The stages were controlled by a Stepnet ST3 controller (figure 26) which could be configured and controlled by a computer through a regular RS232 port [60]. The automated movement of the stage was enabled by ASCII commands sent via the computer or direct usage of commands through CME2 software by Copley Controls. The primary use of the CME2 software is to configure the stepper motors, however it was also used to provide movement of the stages in the X, Y and Z directions. A feature of providing acceleration to the stages in any direction is also available.

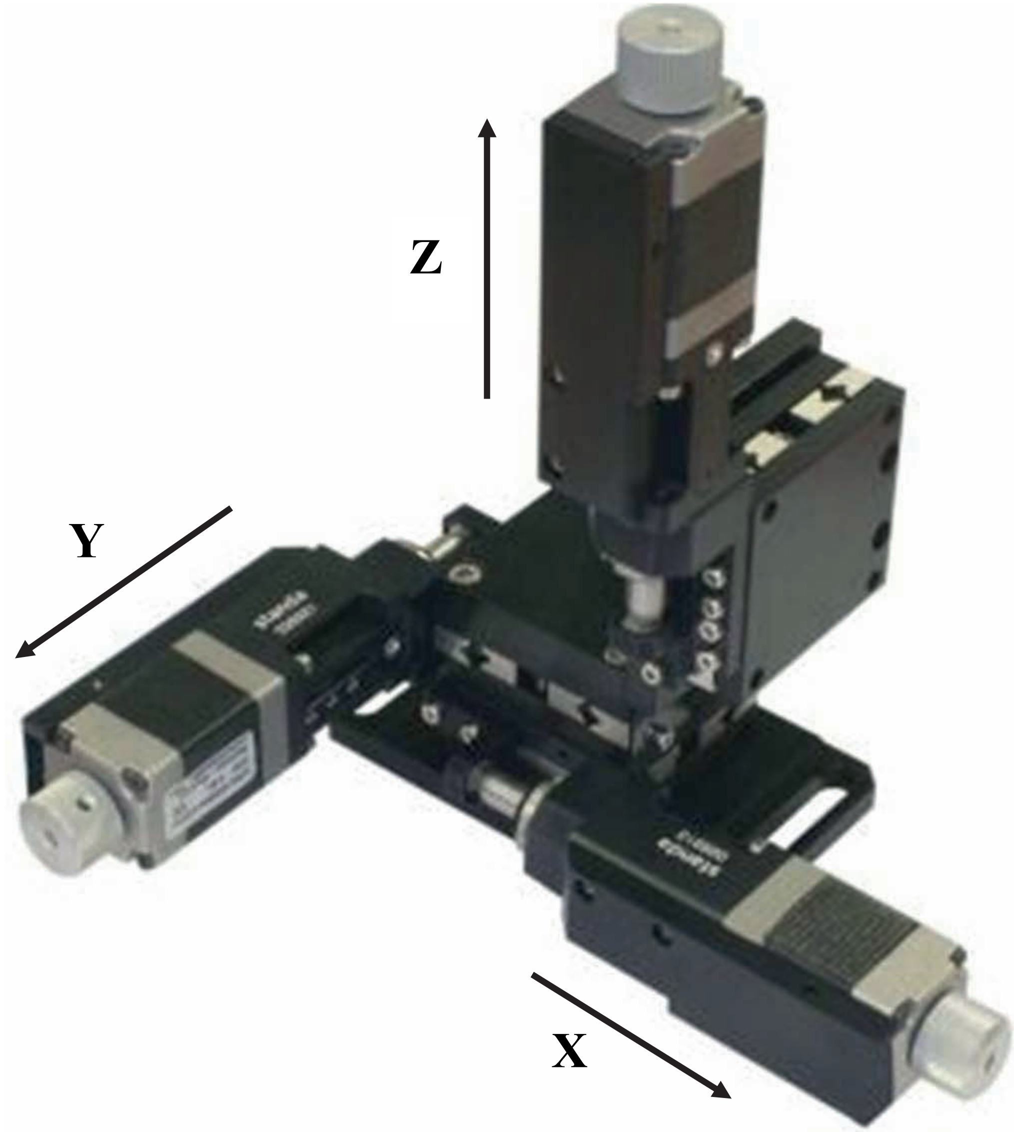

Figure 25 - XYZ-LSMA 184 Stage

Figure 26 - Stepnet ST3 controller [60]

3.4. DμP(R) series W/Microstar pulse power supply

The Dynatronix pulse series DuPR with MicroStar interface are peak voltage or current regulating, pulse reversing and dual level power supplies. Some standard features of the pulse rectifier include an ampere-time totalizer; a voltage/current limit indicator; built-in calibration, fault detection circuitry, real time control and ampere-time control with local alarm. This model has a 6 A peak current at a 10V voltage. Power supply is controlled and monitored through the convenient and simple to use front panel MicroStar keypad. The DμPR series utilizes bipolar (periodic reverse) waveforms which can use a pulse range of 0.1 ms to 99.99 ms (.01 ms resolution).

Some of the advantages of this system are:

- Provides the capability to use bipolar pulses
- Can be connected to a computer via a USB port connection
- Ability to log all the current, voltage data in the system through the computer
- Ability to make and store various setups or combinations of parameters
- Various modes of power supply – Constant voltage mode, constant current mode and crossover current mode (mix of constant voltage and constant current mode)

An image of the pulse rectifier is shown in figure 27. The whole device can be controlled by a computer through a software *Front Panel Plus*. Also, the ability to store setups makes it easy to use specific combinations even for future purposes. The ability to use a pulsed supply at a constant current mode is an additional feature of the system.

Figure 27 - Pulse rectifier

3.5. DM 2400 CNC milling machine

The spindle motor of the DM 2400 CNC milling machine was used to hold and provide rotation to the micro tool through a collet and a sleeve. The motor is a 0.5 HP DC motor with an RPM range from 0 to 5000. A spindle OFF/ON switch is used to control the power to the motor. There is a rotating knob which allows the spindle rotation to vary from the lowest to the highest revolution speed. A rotational effect to the micro tool electrode is crucial for effective and successful micromachining to take place. Primarily, the rotation is used to get axisymmetric machining of anode. It also gives a flushing effect in the machining zone and helps clear out the debris particles and lets fresh electrolyte move in to the vicinity of the anode.

A Dyna Mechatronics collet with a variable diameter from 0.5 to 1 mm a sleeve of internal diameter of 300 µm is also attached to this collet in order to hold the smaller set of 300 µm micro tools.

3.6. Electrodes and Electrolytes

There were two electrode materials used in this research, stainless steel and tungsten rods. The stainless steel electrode was 1 mm in diameter and was fitted in directly in the collet. This material was primarily used for the purpose of a feasibility study of the tool fabrication process. The other electrode material used was tungsten which was 300 µm in diameter and was fitted to the spindle through the collet and a sleeve. Some feasibility studies were conducted on tungsten electrode material too. The final high aspect ratio micro tools were developed using the tungsten electrode. Tungsten is known for its high strength and its nature as a passive metal. It is also popular metal in the manufacturing industry especially as applications of probes and filaments. For these reasons tungsten was chosen for the study of high aspect ratio tools. The tool electrode is made the anode for the tool fabrication process. Strips of stainless steel material 100 µm and 500 µm thick were used as the cathode of the system. Electrolytes used were sodium chloride (NaCl) for tool fabrication and sulfuric acid (H_2SO_4) for micro hole and slot machining. Material safety data sheets for these chemicals are provided in Appendix B.

CHAPTER 4

4. Feasibility Studies

This section describes the feasibility studies conducted at the initial stages of the research in order to better understand the effects of process parameters involved. Studies were also conducted on determining the cone angles and the tip radii of the micro tools to be fabricated. Table 2 lists all the experimental conditions used in the feasibility studies.

Table 2 - Feasibility study experimental conditions

Power supply	10V
Anode	Stainless steel rod of 1 mm dia, Tungsten rod of 300 µm dia.
Cathode	0.5mm thick stainless steel plate
Electrolyte	10% sodium chloride (NaCl) solution
Average Current	0.1, 0.2, 0.25, 0.5, 0.75 A
Pulse On-time	0.1 milliseconds
Duty Cycle	Varied from 10 % - 80%

4.1. Stainless Steel Micro Tools

The first set of experiments was conducted with stainless steel rods of 1 mm diameter. These were performed in a constant current mode in which the voltage varies while current remaining constant. The experiment was repeated for 2 sets of stainless steel electrodes at currents of 0.1 A and 0.2 A with duty cycles of 50%, 66.67% and 80%. The tools subjected to 0.2 A were machined for a total of 850 seconds each. The other set of tools were subjected to 0.1 A for a period of 1900 seconds. After the micro tools were machined, further analysis revealed that the tools primarily had cone angles of about 20° to 25° and the smallest tip radii of about 26µm. Figures 28 (a) and (b) show the SEM images of the stainless steel tool tips developed with 0.2 A current and duty cycles of 50% and 80% respectively. Figures 28 (c) and (d) show the SEM images of the tool tips developed with 0.1 A current and duty cycles of 50% and 66.67% respectively. Table 3 shows the tool tip radii and cone angles of the micro tools measured from the SEM images.

Results listed in Table 3 show an increasing trend of the tip radii with duty cycle of the micro tools for the set of electrodes machined with 0.1 A, however, the tip radii remain consistent for those tools developed with 0.2 A current. Similar to the tip radii, the cone angles increase with increase in duty cycle for the set of tools made with the 0.1 A current, while the cone angles more or less remain constant for micro tools developed with 0.2 A current. It can be concluded that machining with 0.1 A current has a significant impact on the micro tools.

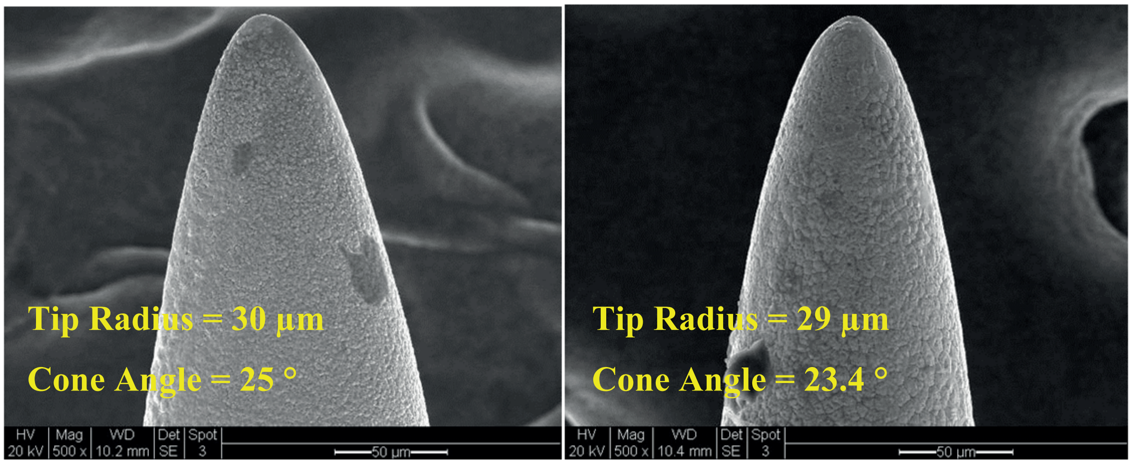

(a) Developed at 0.2A, 50% duty cycle **(b) Developed at 0.2A, 80% duty cycle**

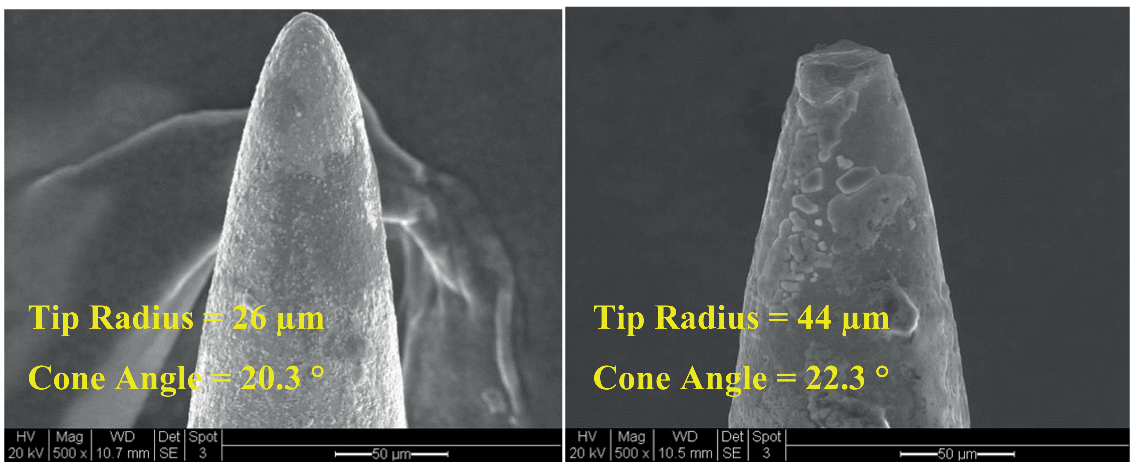

(c) Developed at 0.1A, 50% duty cycle **(d) Developed at 0.1A, 66.67% duty cycle**

Figure 28 - SEM images of Stainless Steel micro tool tips

Table 3 - Feasibility Study of Stainless Steel Micro Tools

Electrode	Average Current (A)	Duty Cycle	Tip Radius (µm)	Cone Angle (°)
1	0.1	50%	26.43	20.3
2	0.1	66.67%	44.76	22.3
3	0.1	80%	61.9	31.3
4	0.2	50%	30.47	25
5	0.2	66.67%	28.81	24
6	0.2	80%	29.04	23.4

4.2. Tungsten Micro Tools

The second set of experiments was conducted with tungsten rods of 300 µm diameter. Tungsten, being a passive metal was machined with pulsed bipolar currents with equal forward and reverse currents of 0.25, 0.5 and 0.75 A. The forward and reverse pulse on-times were at 0.1 ms and were applied at combinations of duty cycles of 10% and 20%. The machined tools had a conical nature of about 2 - 4° taper. The tool tip radii were also measured and tips as small as 50 nm were obtained during this process. Figure 29 shows the SEM image of the tungsten nano-tipped micro tool machined at 10% forward and reverse duty cycle at 0.5 A [61]. The tip radius is found to be 58 nm and the cone angle is found to be 2.5°. Figures 30 (a) and (b) show the SEM images of the tungsten tool tips developed at 0.25 A each with a 20% forward and 20% reverse duty cycle and a 10% forward and 20% reverse duty cycle respectively [61]. Table 4 lists the preliminary study of the tungsten micro tools showing the cone angles and the tip radii of the various micro tools under the different conditions.

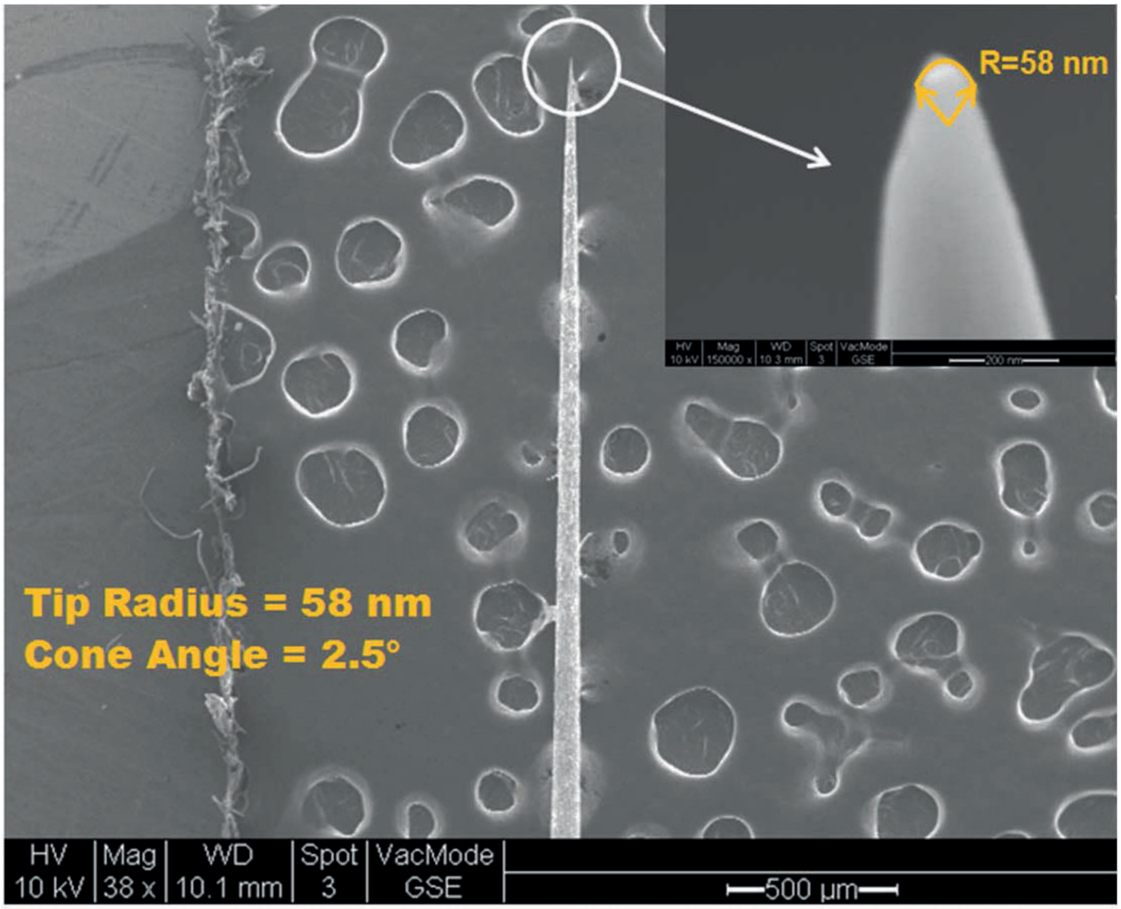

Figure 29 - Micro Tool with conical tip: 10% forward and reverse duty cycle, 0.5A, 0.1ms pulse on-time [61]

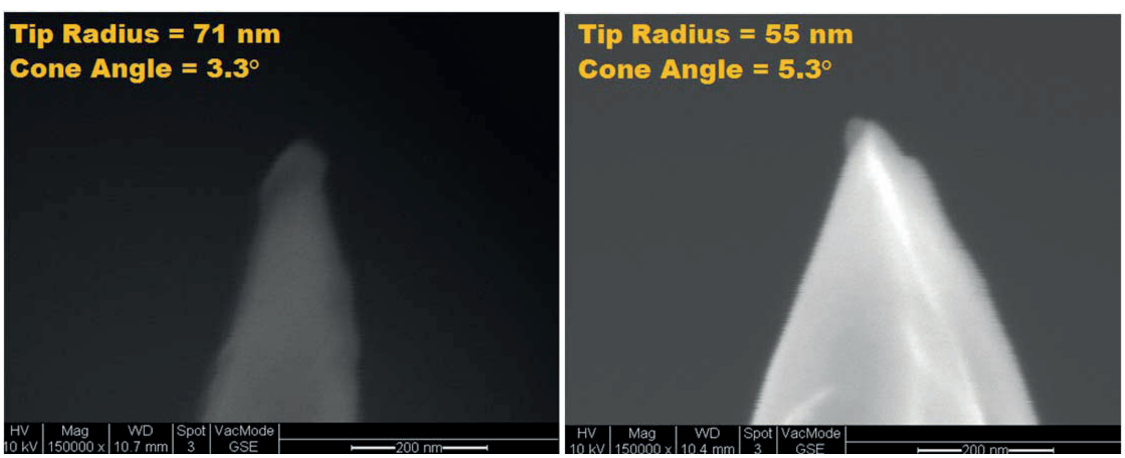

(a) **(b)**

Figure 30 - SEM images of micro tool tips. (a) 20% forward and reverse duty cycle, 0.25A and 0.1ms pulse on-time, (b) 10% forward and 20% reverse duty cycle, 0.25A and 0.1ms pulse on-time [61]

Table 4 - Feasibility Study of Tungsten Micro Tools

Electrode	Average Current (Amps)	Forward Duty Cycle	Reverse Duty Cycle	Time (s)	Tip Radius (nm)	Cone Angle (°)
1	0.25	10%	10%	3375	61.29	3.03
2	0.25	10%	20%	2150	54.83	5.27
3	0.25	20%	20%	1925	70.96	3.27
4	0.5	10%	10%	1075	58.06	2.57
5	0.5	10%	20%	735	225.8	4.91
6	0.5	20%	10%	1325	109.7	3.95
7	0.5	20%	20%	450	86.5	3.24
8	0.75	10%	10%	1050	1005	8.62
9	0.75	10%	20%	630	17900	7.74
10	0.75	20%	10%	1450	279	6.12
11	0.75	20%	20%	465	705	5.2

Table 4 suggests that to fabricate micro tools with lower tip radii, it is favorable to machine at lower currents such as 0.25 A. For most of the tools, there is only a negligible difference between the cone angles of the tools machined in 0.25 A and 0.5 A currents. However, there is a significant rise in cone angles in the case of 0.75 A in all the combinations of the duty cycles. This observation suggests that in order to make micro tools with a lower cone angle, it is favorable to machine at lower currents such as 0.25 A and 0.5 A. Shown in figure 31 is a plot of the tool tip cone angles and the currents they were developed at. Clearly, a large rise in the cone angle values can be seen in the case where the tools were developed at 0.75 A.

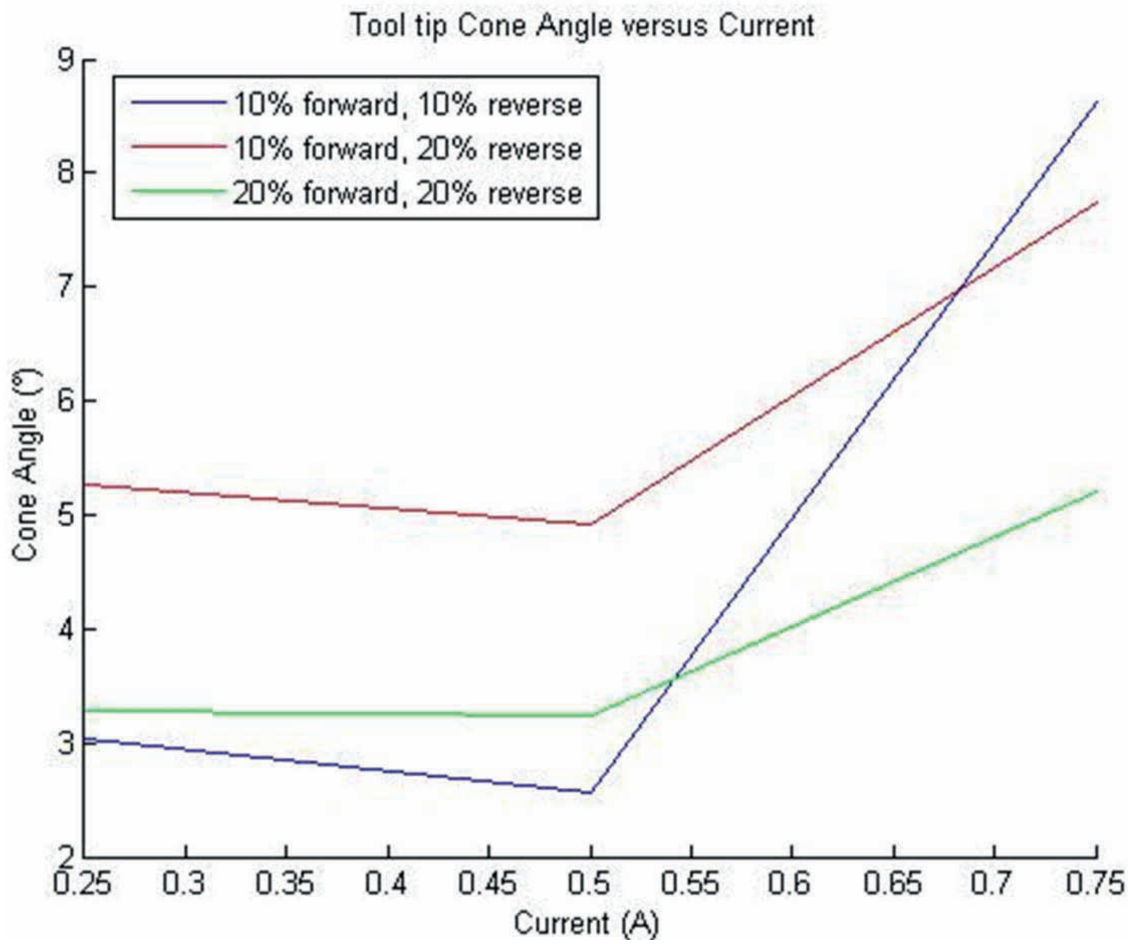

Figure 31 - Plot of Tool tip Cone Angles versus Current

Thus the preliminary studies reveal that:

- The use of lower currents (as 0.25 A) are preferable for smaller tip radii and cone angles.
- With lower currents, lower duty cycles are more preferable for smaller tip radii and cone angles.
- Tools had a small tip radii (~50nm) and were conical in nature

CHAPTER 5

5. Mathematical Modeling

This section describes a mathematical model developed to predict the anodic profile for tool electrode fabrication in the micro ECM process. The effect of a moving cathode on the interelectrode gap is used to predict the final diameter formed under different velocities of the cathode movement.

5.1. Model Development

This model discusses the effect of the velocity of the cathode on the final diameter of the tool electrode (anode) in terms of the interelectrode gap and the pulse on-time. A mathematical model is developed to build a relation between the final diameter of the anode and the velocity of the cathode. Shown in figure 32 is a two dimensional representation of the electrodes in a micro ECM system. The anode has an initial diameter D_i and a cathode of width W is kept at an initial interelectrode gap S_0. The cathode moves up in the Z axis along the tool with a velocity V. This model uses the interelectrode gap to formulate the final diameter of the tool D_f in terms of this velocity V.

Some of the assumptions used in this model are:

- Heat and bubble generation effects neglected.
- Current Efficiency η, over potential ΔU, electrolyte conductivity κ_e are considered to be constant.
- Only surfaces normal to the cathode undergo machining i.e. no machining occurs on the sides of the normal surfaces.

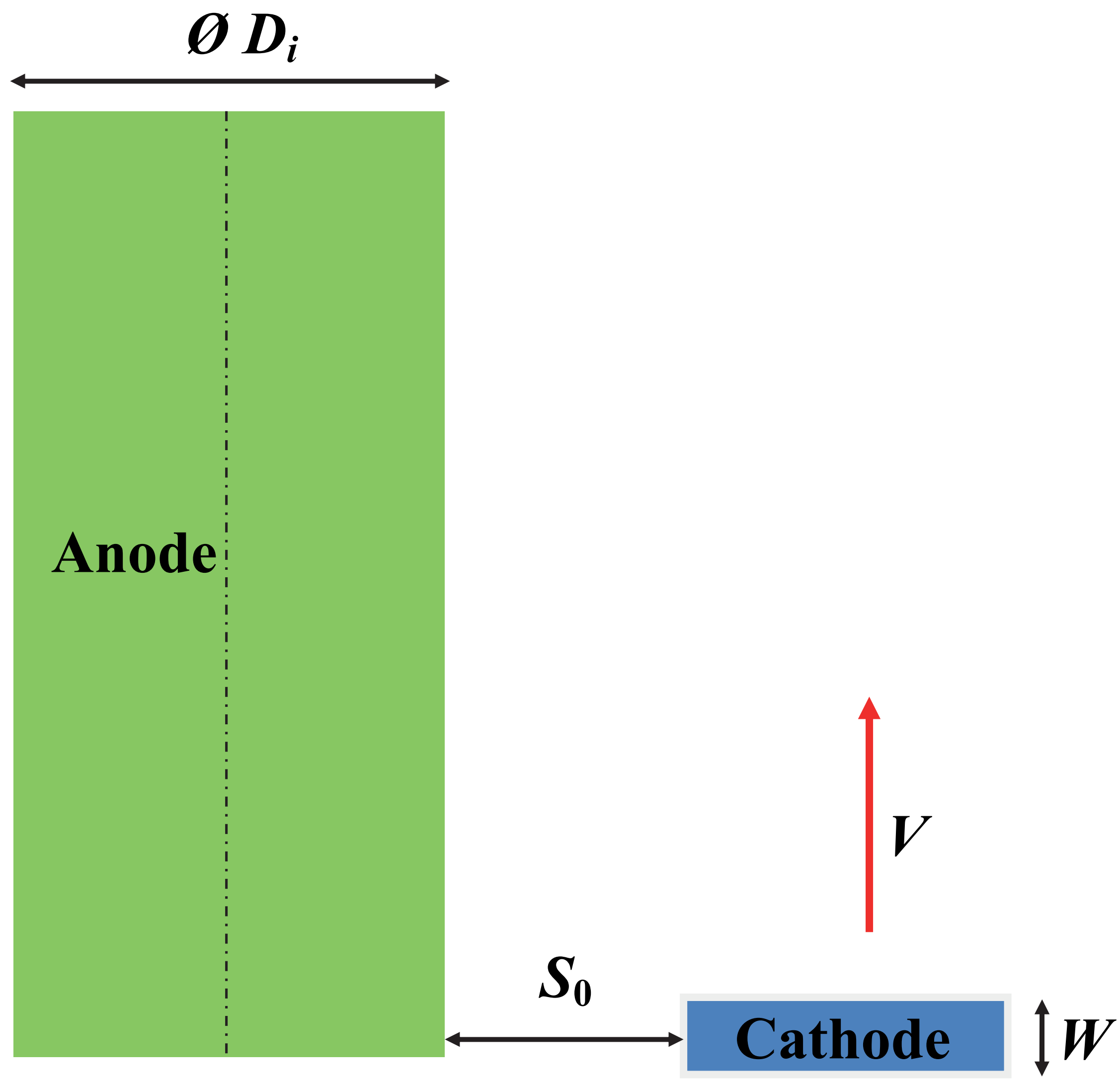

Figure 32 - Modeling the interelectrode gap during tool fabrication

For any small element on the anode, the anodic dissolution rate $\dot{r}_a$ can be expressed as the change in the interelectrode gap as [24, 58]:

$$\dot{r}_a = \frac{dS}{dt} = \frac{\eta \kappa_e k_v (U_0 - \Delta U)}{S} \quad (1)$$

Where η is the current efficiency of anodic dissolution, κ_e is the electrolyte conductivity, k_v is the volumetric electrochemical equivalent, S is the inter-electrode gap, $U_0$is the applied voltage and ΔU is the over potential value. For any small element on the anode normal to the cathode, it will undergo machining during the pulse on time. This equation can be integrated over a time period of a single pulse (0 - t_p) to give the equation of gap after a single pulse [58]. Integrating for a pulse on time of t_p

$$S_1 = \sqrt{{S_0}^2 + 2\eta\kappa_e k_v(U_0 - \Delta U)t_p} \ldots\ldots\ldots\ldots\ldots\ldots\ldots\ldots\ldots\ldots (2)$$

Where S_0 is the initial gap at time $t = 0$, S_1 is the gap after one pulse. This equation gives the gap after 1 pulse.

Now for the second pulse on time,

$$S_2 = \sqrt{{S_1}^2 + 2\eta\kappa_e k_v(U_0 - \Delta U)t_p} \ldots\ldots\ldots\ldots\ldots\ldots\ldots\ldots\ldots\ldots (3)$$

Substituting the value of S_1 from equation (2) in (3),

$$S_2 = \sqrt{{S_0}^2 + 2\eta\kappa_e k_v(U_0 - \Delta U)t_p + 2\eta\kappa_e k_v(U_0 - \Delta U)t_p}$$

$$S_2 = \sqrt{{S_0}^2 + 4\eta\kappa_e k_v(U_0 - \Delta U)t_p}$$

Where, S_2 is the gap after the second pulse. Thus, the gap after m pulses is

$$S_m = \sqrt{{S_0}^2 + 2m\eta\kappa_e k_v(U_0 - \Delta U)t_p} \ldots\ldots\ldots\ldots\ldots\ldots\ldots\ldots\ldots\ldots (4)$$

Now, let the cathode of width W move along the infinitesimally small element of the tool (anode) with a velocity of V in a time t as shown in figure 33. Let the total number of pulses that impact that small length of the tool be m. The total number of pulses m is the product of pulse rate (number of pulses per second) p and the time spent under the cathode t. Thus,

$$m = p \times t$$

The time *t* is given by a simple distance by velocity equation:

$$t = \frac{W}{V}$$

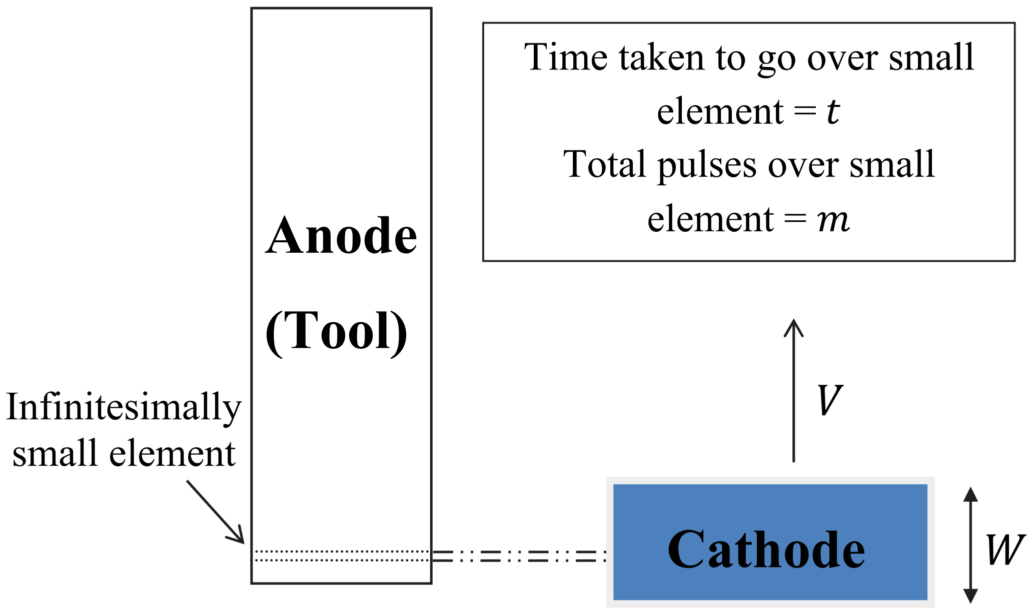

Figure 33 - Mathematical Model Description

Thus m can be expressed as

$$m = \frac{p \times W}{V} \qquad (5)$$

Substituting the value of m from equation (5) into (4):

$$S = S_m = \sqrt{{S_0}^2 + \frac{p \times W}{V} 2\eta\kappa_e k_v (U_0 - \Delta U) t_p} \qquad (6)$$

Equation (6) represents the final gap S. The radial amount of tool material machined is essentially the change in gap,

$$\Delta S = S - S_o \qquad (7)$$

Due to the rotation of the tool, the final diameter can be obtained by subtracting twice the final gap from the initial diameter.

$$D_f = D_i - 2\Delta S \qquad (8)$$

Substituting the value of ΔS, from equation (7) in (8)

$$D_f = D_i - 2(S - S_o) \qquad (9)$$

Finally, substituting the value of $S, ie., S_m$ from equation (6) in (9) a mathematical model given below is obtained to predict the final diameter D_f of the anode in terms of the initial diameter D_i, the initial interelectrode gap S_0, pulse on-time t_p and the velocity of the cathode V.

$$D_f = D_i - 2(\sqrt{{S_0}^2 + \frac{p \times W}{V} 2\eta\kappa_e k_v (U_0 - \Delta U) t_p} - S_0)$$

5.2. Experimental Verification of the Model

The model developed above uses two material specific constants, a system efficiency factor, and several user specified experimental values. The material specific constants are the volumetric electrochemical equivalent of tungsten $k_v = 1.65 \times 10^{-11}$ m^3/As, and conductivity of sodium chloride κ_e = 20 A/Vm. The system efficiency η was experimentally determined as 0.49. The user specified experimental values are the applied voltage U_0= 10V, overpotential ΔU= 0V, a duty cycle D of 33%, cathode width W = 100 µm, pulse rate p = 66.67, pulse on time t_p = 5.0 ms, and initial diameter D_i = 300 µm, and cathode velocity V.

Now, using the above mentioned values, for the cathode velocity of 3.6 µm/s and 2.7 µm/s, the theoretical model predicts the final diameter of the anode to be 100 µm and 53 µm respectively. Verification results obtained from experiment is shown in figure 34. A comparison of theoretical and experimental values of anode diameters is shown in figure 35. It can be seen that the model developed is able to predict the diameter of the ECM machined shaft within 6 to 17 % variation.

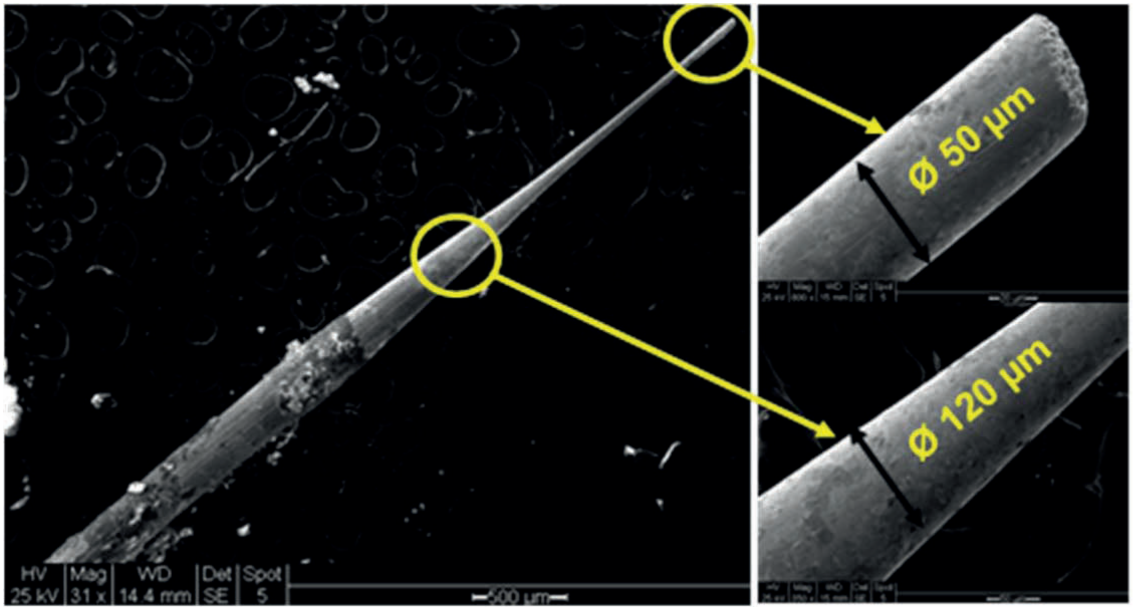

Figure 34 - Experimental verification

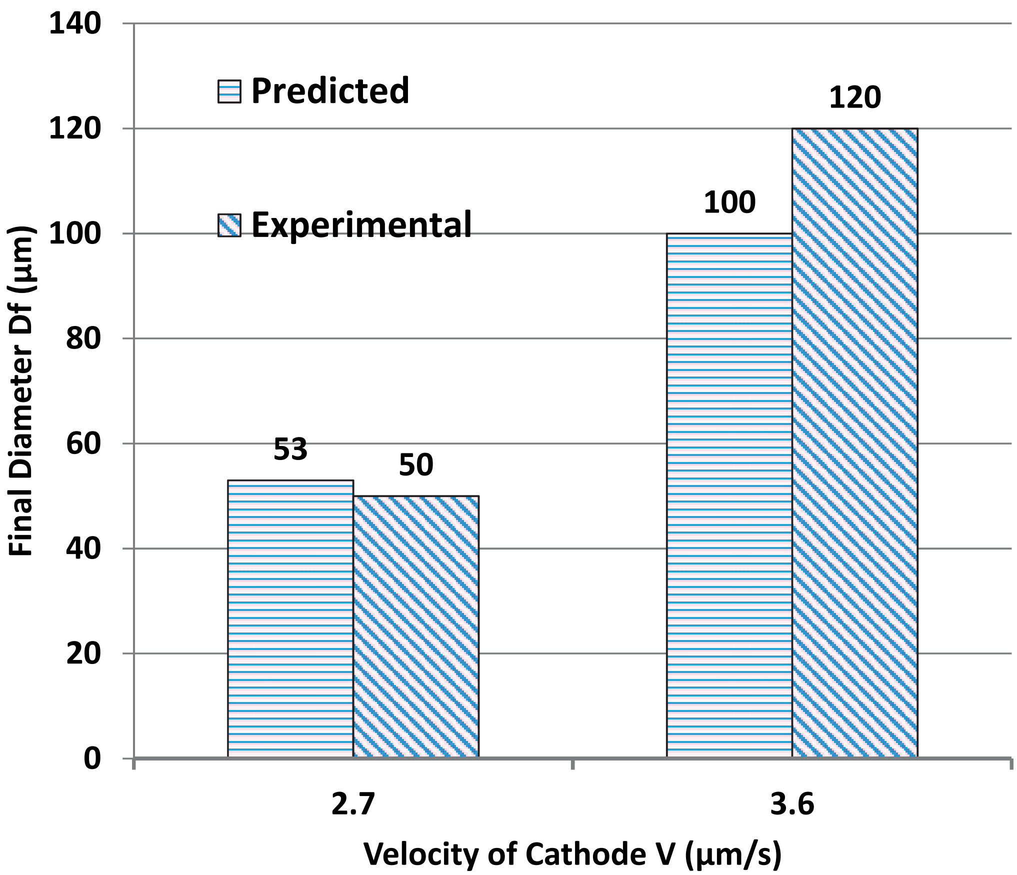

Figure 35 - Comparison of predicted and actual diameters

CHAPTER 6

6. Machining of Ultra High Aspect Ratio Micro Tools

A picture of the experimental setup is shown in figure 36. The electrolytic tank holding the cathode is filled with the electrolyte and is mounted on an X-Y stage which can provide the motion in the longitudinal and lateral directions. The spindle holding the anode is attached to the Z stage which feeds the anode in the vertical direction. The pulse rectifier connects to both the anode and the cathode and provides the required current and voltage for machining. After the anode is positioned with respect to the cathode, the rectifier is turned on and used at a constant current mode. The constant current mode enables the system to keep a fixed current and vary the voltage as the tool moves relatively to the cathode. The pulse rectifier used in this case supplied up to 10V of voltage.

Table 5 lists the experimental parameters used in this process. The overall process flow chart is shown in figure 37. The required parameters are input into the pulse rectifier and then machining takes place. Once the machining is done, the micro tool is removed and a Scanning Electron Microscope (SEM) image is taken for further analysis or the polarity on the pulse rectifier can be reversed and machining operations on the cathode can be conducted.

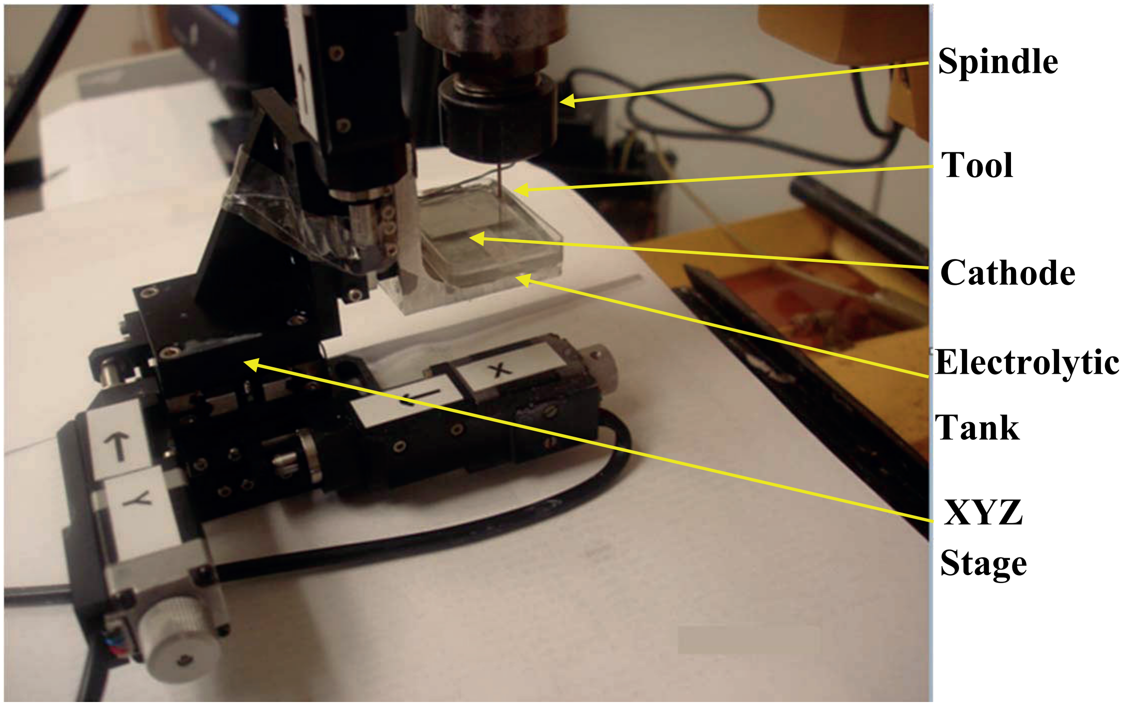

Figure 36 - Experimental Setup

Table 5 - Experimental Conditions

Power supply	0-10V DC
Anode	Tungsten rod of 300 μm dia.
Cathode	Stainless steel strip of 0.5mm thick
Electrolyte	10% Sodium Chloride (NaCl) solution
Average Current	0.25, 0.5, 0.75 A
Pulse Time	0.1 - 10 milliseconds
Duty Cycle	10 %, 20% and 33%

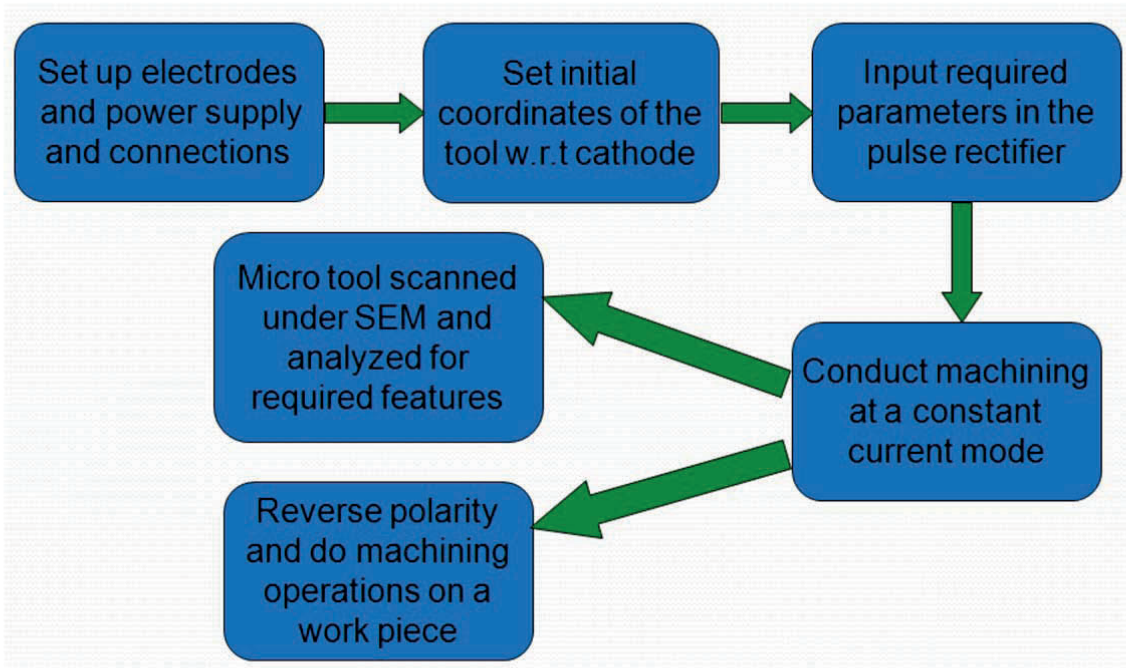

Figure 37 - Overall process flow chart

6.1. High Aspect Ratio Tool Fabrication

Experiments were conducted to achieve high aspect ratio tools. Using the Ø 300 µm tungsten micro electrodes, the set of tools are treated with bipolar currents of equal forward and reverse currents of 0.25A. The pulse on-times were varied from 1 to 10 ms and the duty cycles used were 10%, 20% and 33%. These samples were observed under a Scanning Electron Microscope (SEM). The results and discussions are presented in the following section.

This set of experiments were done by applying pulses with pulse on-time beyond 1 ms up to 10 ms and highly cylindrical micro tools are machined. Figure 38 shows an SEM image of a high aspect ratio micro tool developed at 5.0 ms pulse on-time and 33% duty cycle (forward and reverse) [61]. The tungsten tool has a length of 2.8 mm with a diameter of 10 micrometers giving a high aspect ratio of 280.

Table 6 shows the aspect ratio (length / diameter) of these micro tools with varying pulse on-times of 1 ms and 5 ms and duty cycles of 10%, 20% and 33% [61]. It clearly shows that at a pulse on-time of 5 ms, the aspect ratios achieved are much higher than those developed at 1 ms pulse on-time. Also, another observation was that it was more successful in obtaining larger lengths of the anode on application of lower duty cycles such as 10%.

Figure 39 shows an ultra high aspect ratio tool developed with a total length of 4.5 mm and a diameter of about 10 micrometers, giving an aspect ratio of 450. Since the tool was too long, it has been imaged in two sections - AB and BC. By varying the diameter in steps, even longer tools can be micro machined, figure 40 shows a stepped shaft developed at 7.5 ms pulse on-time made of 3 steps – AB, BC and CD. Table 7 lists the lengths, diameters and aspect ratios of the 3 steps of the stepped shaft in figure 40.

Similar higher aspect ratios were obtained when the pulses were raised to 7.5 to 10 ms pulse on time. However, as the pulse on-time rises, it results in a reverse conical shape. Figure 41 shows a micro tool developed at 0.25 A and 20 ms pulse on-time which results in a reverse conical shape of the anode [61]. A higher pulse on-time corresponds to higher energy input as in the case of application of a large current density and voltage that has been reported to form a reverse conical shape tool in [44].

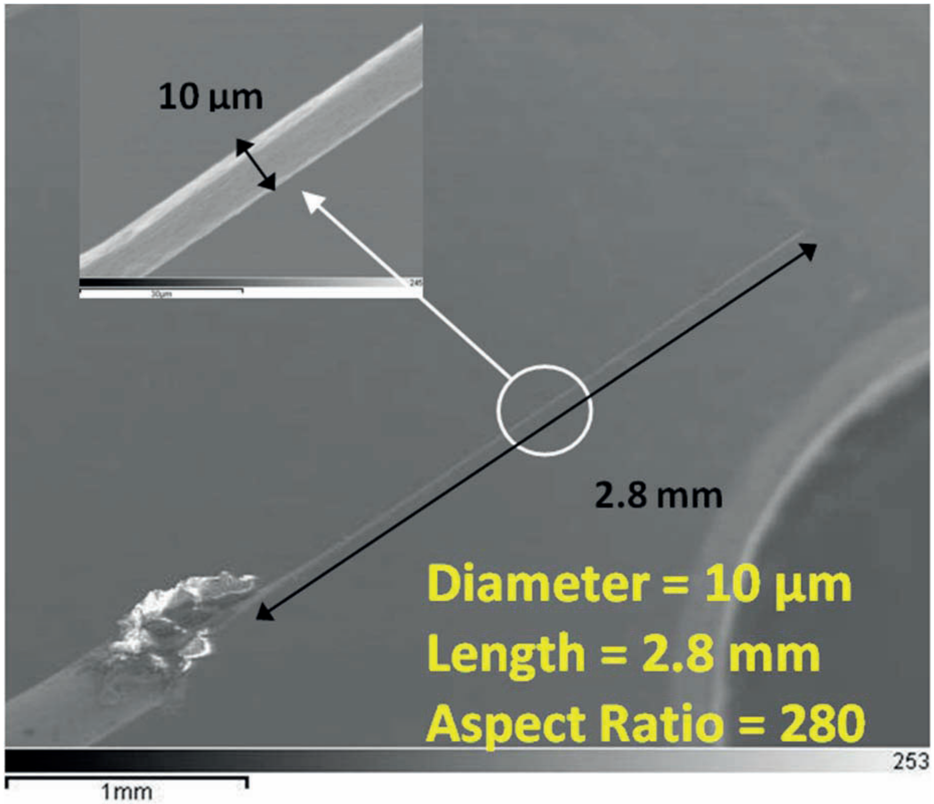

Figure 38 - High Aspect Ratio Tungsten Micro Tool: 5.0 ms pulse, 33% forward and reverse duty cycle [61]

Table 6 - Study of High Aspect Ratio Tools [61]

Electrode	Pulse On-Time	Duty Cycle (Forward & Reverse)	Time (s)	Diameter (µm)	Length (µm)	Aspect Ratio (length : diameter)
1	1.0	10%	1135	29.0	2500	86
2	1.0	20%	610	21.73	2043	94
3	1.0	33%	305	18.3	2158	118
4	5.0	10%	1985	11.08	3254	294
5	5.0	20%	990	14.5	3284	227
6	5.0	33%	563	9.85	2776	282

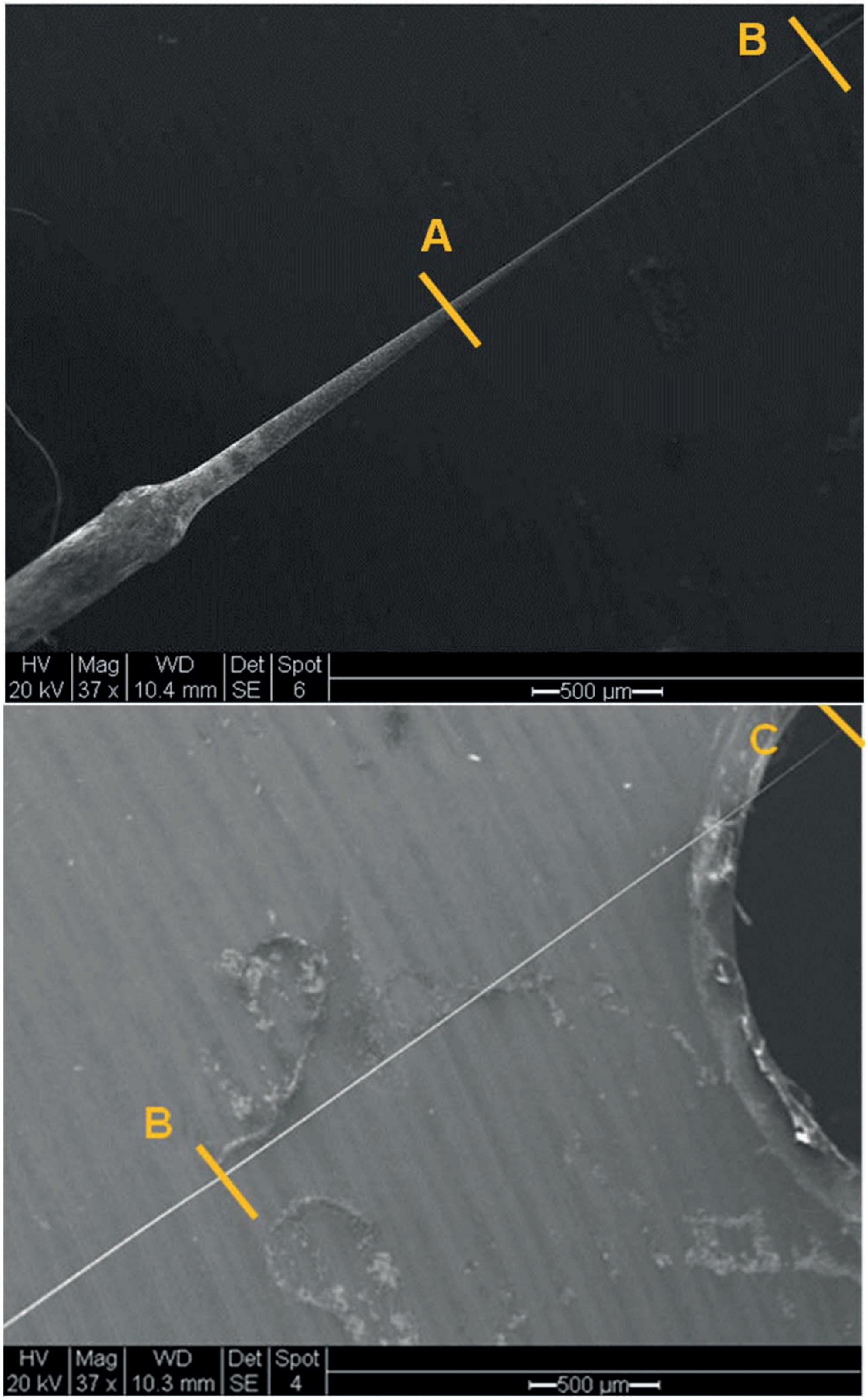

Figure 39 - Ultra high aspect ratio micro tool of length of 4573µm, diameter of 10µm and an aspect ratio of 450

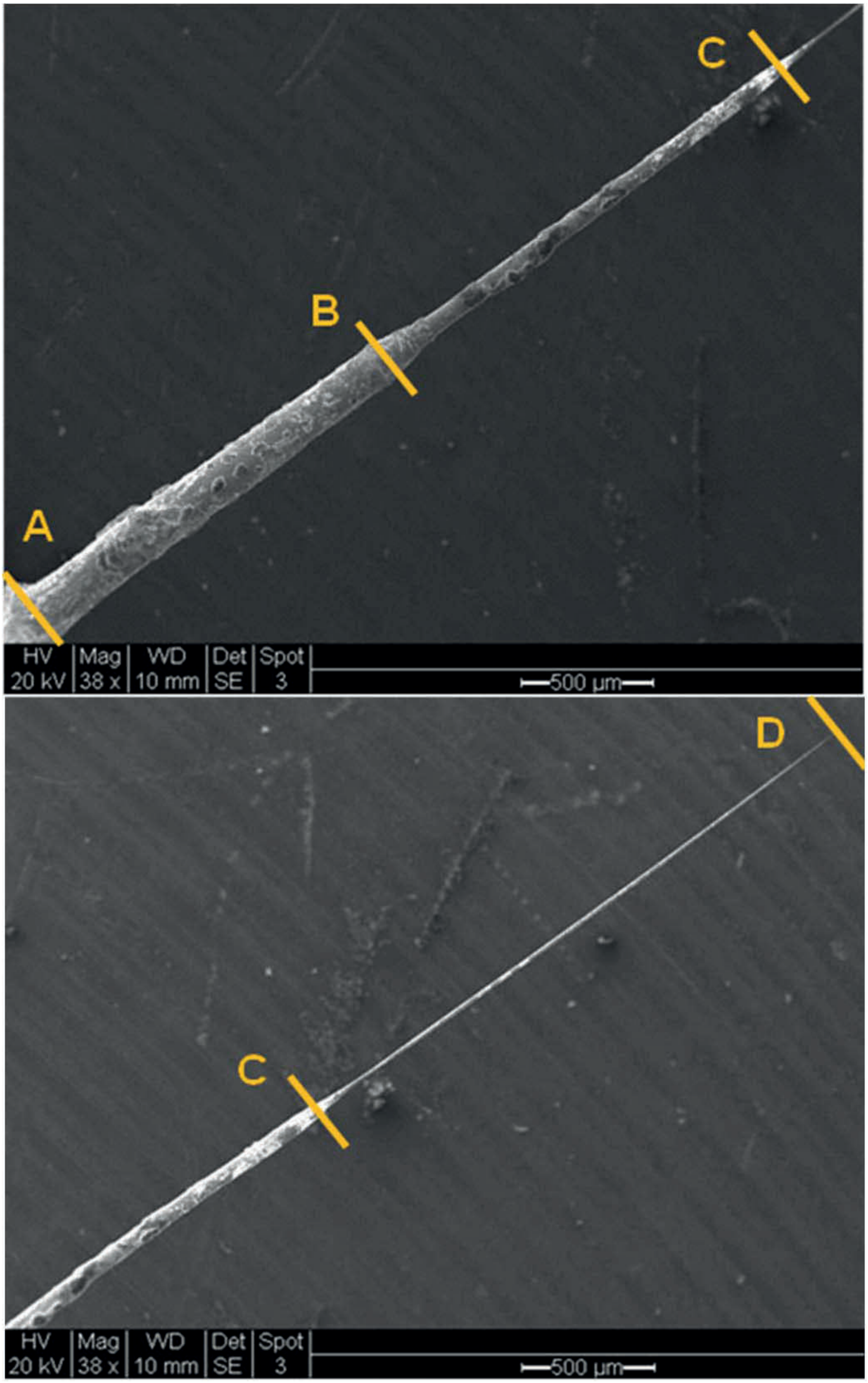

Figure 40 - Stepped shaft developed with large 7.5 ms pulse on-time

Table 7 - High aspect ratio stepped shaft

Section	AB	BC	CD
Length (μm)	1540	1860	2360
Diameter (μm)	196	70	14
Aspect Ratio	8	27	169

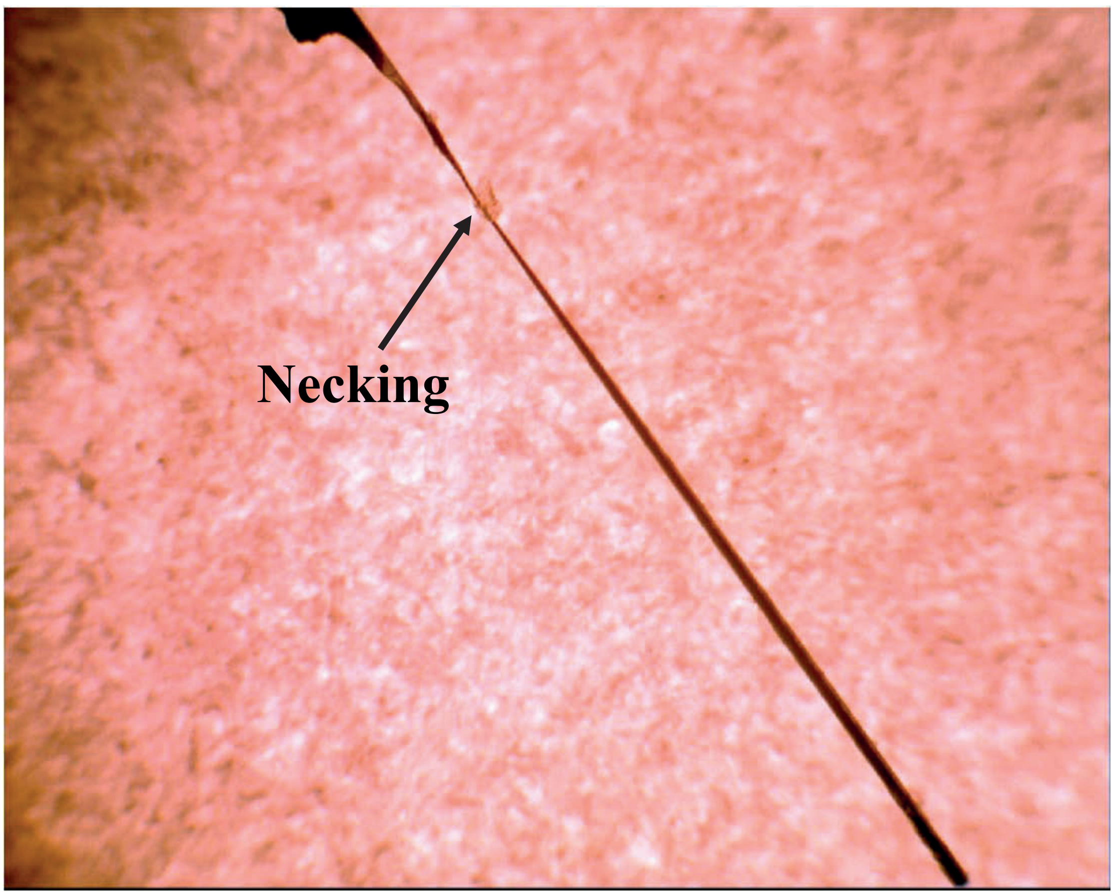

Figure 41 - Reverse conical shape for micro tool developed at 20 ms pulse on-time [61]

6.2. Micro Hole Drilling and Micro slot Machining

For all the micromachining purposes, the electrolyte used was 1.0 M H_2SO_4 acid. Figure 42 shows a micro slot on a 914 µm thick SS plate. This slot was machined at a 6V voltage, 60 µs pulse on-time, 1% duty cycle and a 0.4 µm/s feed. It had a width of 90 µm and a length of about 234 µm. Figure 43 shows a through micro hole in a stainless steel plate of 914 µm thickness. It was drilled at a 60 µs pulse on-time with a voltage of 5V and a duty cycle of 5%. A vertical feed of 0.5 µm/s was provided for the drilling application. The entry hole measures a diameter of about 437.5 µm while the exit hole diameter measures a diameter of about 359 µm. Taking the total depth of 914 µm into account, it gives a taper angle of about 4.9° and an aspect ratio of 2.5. Figure 44 shows a micro hole through a 100 µm SS plate, with a pulse on-time of 250 ns, 2.5 µs pulse period and a 5V voltage and a feed rate of 0.4 µm/s . The diameter of the hole is found to be 138 µm.

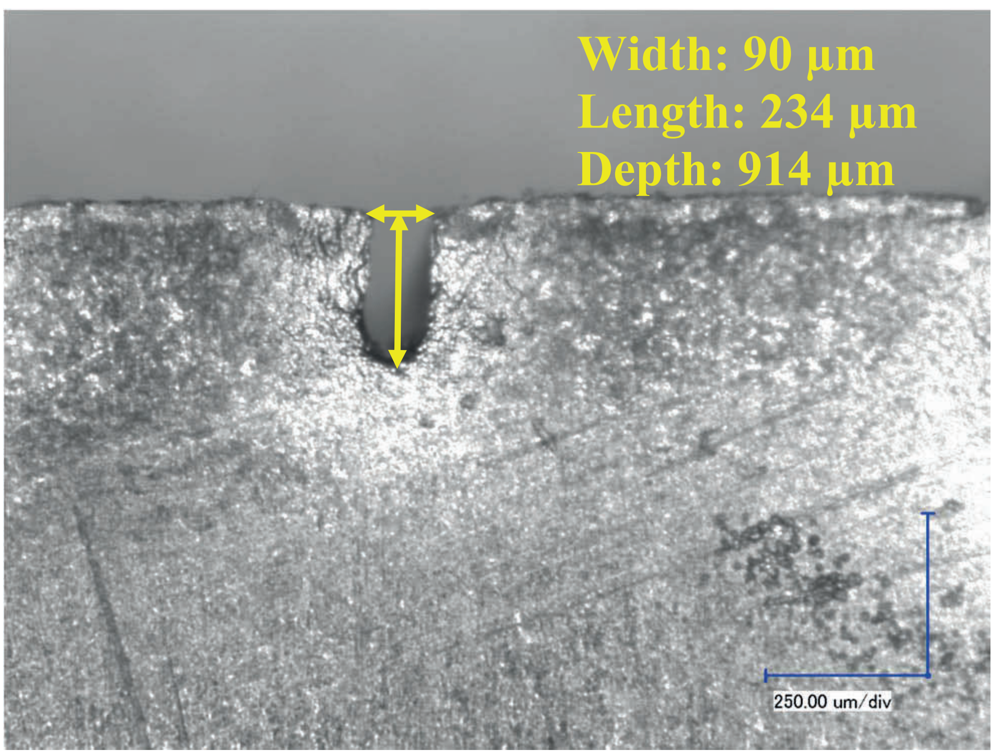

Figure 42 - Micro slot in a 914 µm SS plate, 89.84 µm wide and 234.37 µm long

(a)

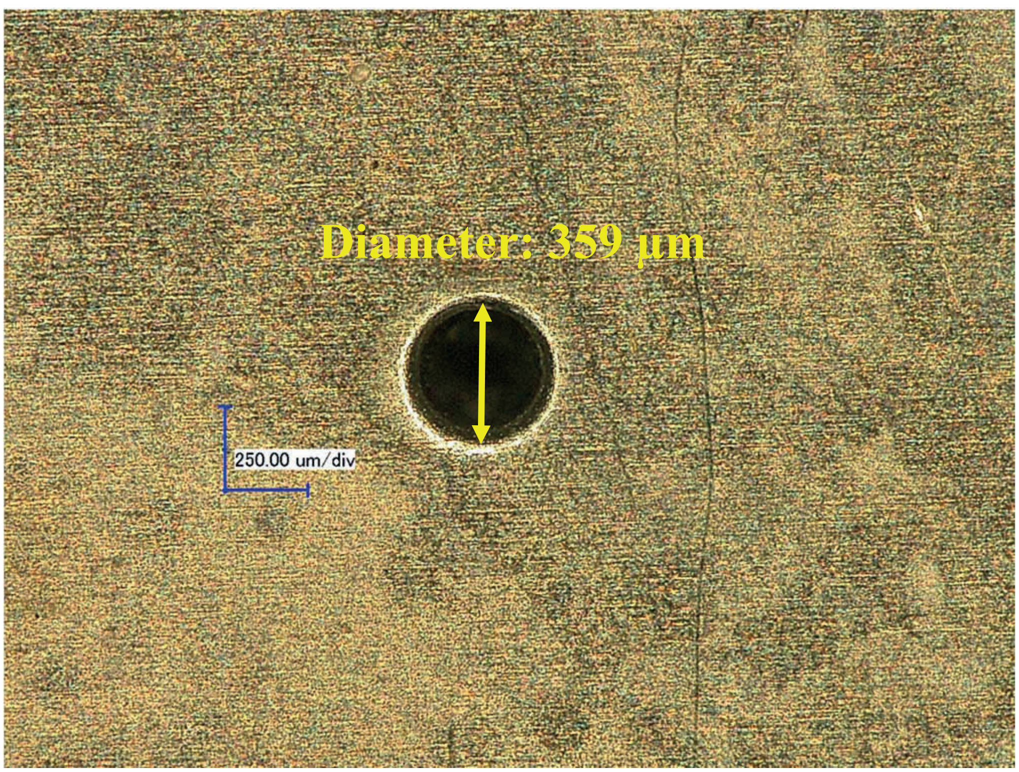

(b)

Figure 43 - Through micro hole on a 914 µm thick SS plate. Diameter of (a) Entry hole: 437.5 µm (b) Exit hole: 359 µm

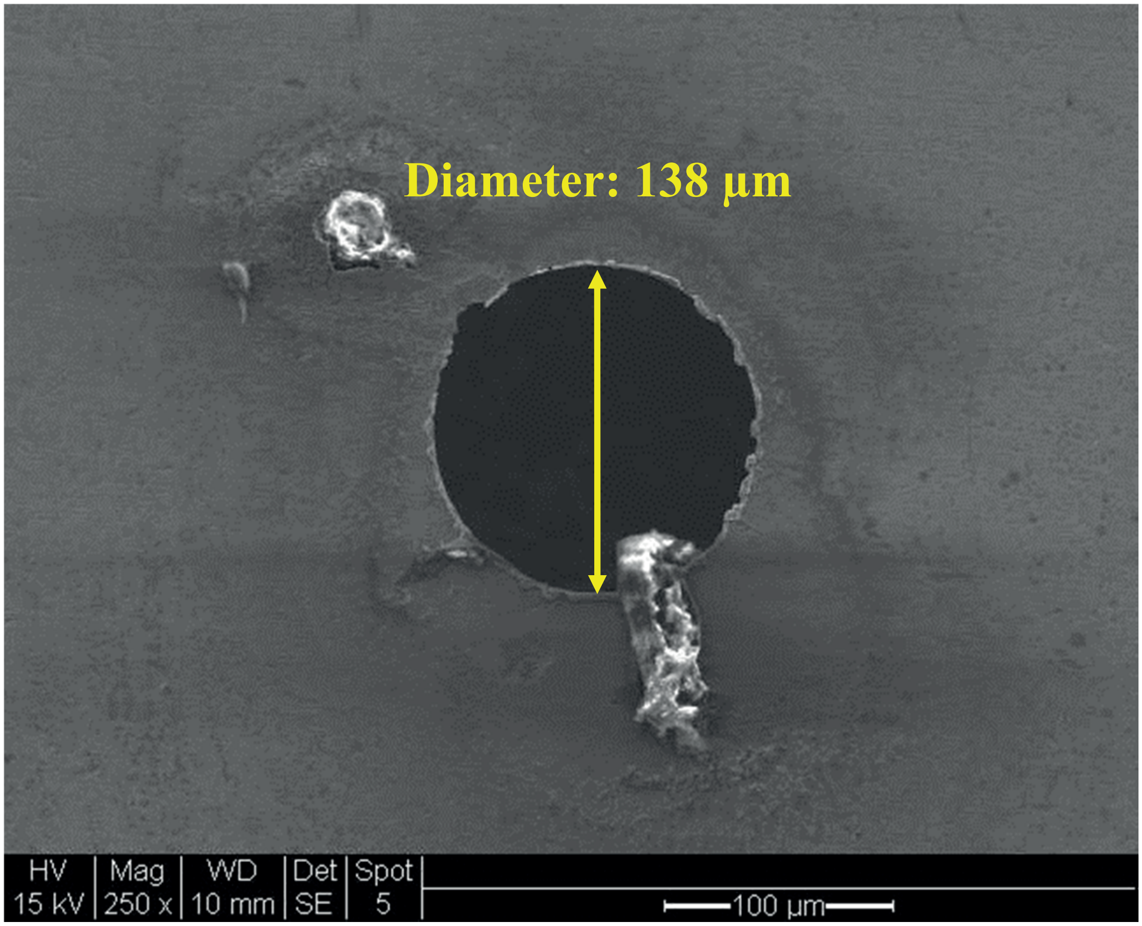

Figure 44 - Through micro hole on a 100 µm SS plate. Hole Diameter is 138 µm at a pulse on-time = 250 ns, feed rate = 0.4 µm/s.

CHAPTER 7

7. Conclusions and Future Work

A micro electrochemical machining system was designed and built in-house in this study. A mathematical model using the interelectrode gap has been developed to predict the final diameter of the anode using the velocity of the cathode. The final diameter of the tool increases with the increase of the velocity of the cathode. Experimental verification of the model reveals that this model is capable of predicting the final diameter of the tool within 6 to 17% variation.

Extremely high aspect ratio micro tools have been successfully fabricated using the in-house built pulsed micro electrochemical machining system. Lower pulse on-times tend to produce micro tool electrodes of a more conical nature, thus, the use of larger pulse on-times for the fabrication of tool electrodes is suggested. Using pulse on-times of 5 to 10 ms, long thin cylindrical micro tool electrodes can be fabricated. It was also noticed that as pulse on-times increase beyond this optimum range, there is a tendency to form reverse conical shaped tool.

Using of higher pulse on-times of 5 to 10 ms, tools with aspect ratios of 450 have been fabricated with diameters of 10 micrometers and length of over 4.5mm. By varying the diameter in steps even longer tools can be micro machined.

Future work can include the implementation of a 3 dimensional mathematical model for micro electrochemical tool fabrication system. As a follow-up of the present study, a mathematical approach based on first principles needs to be carried out to determine the optimum range of pulse on-time for ultra high aspect ratio micro tool fabrication by electrochemical machining. The application of these high aspect ratio tools to machine high aspect ratio holes will be an important extension of the present work.

REFERENCES

1. Fujita H., *Microactuators and micromachines.* Proc. IEEE, 1998. 86: p. 1721-32.
2. Dario P., Carrozza M.C., Croce N., Montesi M.C., and Cocco M., *Non-traditional technologies for microfabrication.* J. Micromech. Microeng., 1995. 5: p. 64-77.
3. Petersen E.K., *Silicon as a mechanical material.* Proc. IEEE, 1982. 70(5): p. 420-457.
4. Rajurkar K.P. and Sundaram M.M., *Overview of Micromachining Processes.* Proc Int. Conference on Trends in Product Life Cycle - Modeling, Simulation and Synthesis, 2006. PLMSS06.
5. Benedict G.F., *Nontraditional Manufacturing Processes.* 1987.
6. Clifton D., Mount A.R., Alder G.M., and Jardine D., *Ultrasonic measurement of the interelectrode gap in electrochemical machining.* Int J Mach Tools Manuf, 2002. 42: p. 1259-1267.
7. Sundaram M.M. and Rajurkar K.P., *Chapter 6 Electrical and Electrochemical Processes* Intelligent Energy Field Manufacturing and Interdisciplinary Process Innovations, 2010.
8. Malshe A.P., Rajurkar K.P., Virwani K.R., Taylor C.R., Bourell D.L., Levy G., Sundaram M.M., McGeough J., Kalyanasundaram V., and Samant A.N., *Tip-based nanomanufacturing by electrical, chemical, mechanical and thermal processes.* CIRP Annals - Manufacturing Technology, 2010. 59(2): p. 628-651.
9. Rajurkar K.P. and Yu Z., *3D Micro-EDM Using CAD/CAM.* CIRP Annals - Manufacturing Technology, 2000. 49(1): p. 127-130.
10. Luis C., Puertas I., and Villa G., *Material removal rate and electrode wear study on the EDM of silicon carbide.* Journal of Materials Processing Technology, 2005. 164-165: p. 889-896.
11. Jung T.H., Park K.Y., and Lee W.K., *A study on the micro electric discharge grinding characteristics of WC-Co-relationship between surface integrity and dielectric conditions.* Science and Technology, IEEE, 2000.
12. Liu H., Yan B., Chen C., and Huang F., *Application of micro-EDM combined with high-frequency dither grinding to micro-hole machining.* International Journal of Machine Tools and Manufacture, 2006. 46(1): p. 80-87.
13. Kunieda M., Lauwers B., Rajurkar K.P., and Schumacher B.M., *Advancing EDM through Fundamental Insight into the Process.* Annals of the CIRP 2005. 2(54): p. 599–622.

14. Liu Y., Zhao F., Sundaram M.M., and Rajurkar K.P., *Study on the Surface Integrity of Machined Tool in Micro EDM.* Proceedings of the 16th international symposium on electromachining 2010((ISEM XVI)): p. 685-689.
15. Rajurkar K.P., Zhu D., McGeough J., Kozak J., and Desilva A., *New Developments in Electro-Chemical Machining.* CIRP Annals - Manufacturing Technology, 1999. 48(2): p. 567-579.
16. Bhattacharyya B., *Advancement in electrochemical micro-machining.* International Journal of Machine Tools and Manufacture, 2004. 44(15): p. 1577-1589.
17. Yong L., Yunfei Z., Guang Y., and Liangqiang P., *Localized electrochemical micromachining with gap control.* Sensors and Actuators A: Physical, 2003. 108(1-3): p. 144-148.
18. Bhattacharyya B., *Experimental investigation on the influence of electrochemical machining parameters on machining rate and accuracy in micromachining domain.* International Journal of Machine Tools and Manufacture, 2003. 43(13): p. 1301-1310.
19. Durr U., *Laser drilling in industrial use. Laser Tech* Laser Tech 2008. 1(J 5): p. 57–59.
20. Ifju P.G., Jenkins D.A., Ettinger S., Lian Y., and Shyy W., *Flexible-wing-based micro air vehicles.* AIAA Aerosp. Sci. Meet. Exhibit, 40th, Reno, , 2002. AIAA 2002-0705: p. 1–13.
21. Hanein Y., Schabmueller C.G.J., Holman G., Lucke P., Denton D.D., and Bohringer K.F., *High-aspect ratio submicrometer needles for intracellular applications* J. Micromech. Microeng., 2003 13 (S91).
22. Hangarter C.M., George T., and Myung N.V., *Electrochemically Fabricated Microelectromechanical Systems/Nanoelectromechanical Systems (MEMS/NEMS).* Electrochemical Technologies, Nanostructure Science and Technology, 2010(Part 4): p. 187-226.
23. Urban G., *Microstructuring of organic layers for microsystems.* Sensors Actuators 1999. 74: p. 219–224.
24. McGeough J., *Principles of Electrochemical Machining.* 1974: p. xv, 255.
25. Davydov A. D., Volgin V.M., and Lyubimov V.V.L., *Electrochemical Machining of Metals: Fundamentals of Electrochemical Shaping.* Russian Journal of Electrochemistry, 2004. 40(12): p. 1438-1480.

26. Bhattacharyya B., Doloi B., and Sridhar P.S., *Electrochemical Micro-Machining: New Possibilities for Micro-Manufacturing.* Journal of Materials Processing Technology, 2001. (1–3)(113): p. 301–305.
27. Kozak J., Rajurkar K.P., and Makkar Y., *Study of Pulse Electrochemical Micromachining.* Journal of Manufacturing Processes, 2004. 6(1): p. 7-14.
28. www.electroburr.com. [cited 2011 01/11].
29. Wang M.H. and Zhu D., *Fabrication of multiple electrodes and their application for micro-holes array in ECM.* The International Journal of Advanced Manufacturing Technology, 2008. 41(1-2): p. 42-47.
30. Ryu S.H., *Micro fabrication by electrochemical process in citric acid electrolyte.* Journal of Materials Processing Technology, 2009. 209(6): p. 2831-2837.
31. Kang M., Yang Y., and Fu X.Q., *Study on Numerical Controlled Electrochemical Turning.* Materials Science Forum, 2009. 626-627: p. 351-356.
32. Mahdavinejad R. and Hatami M., *On the application of electrochemical machining for inner surface polishing of gun barrel chamber.* Journal of Materials Processing Technology, 2008. 202(1-3): p. 307-315.
33. Datta M. and Landolt D., *Electrochemical machining under pulsed current conditions.* Electrochemica Acta., 1980. 26(7): p. 899-907.
34. Jo C.H., Kim B.H., and Chu C.N., *Micro electrochemical machining for complex internal micro features.* CIRP Annals - Manufacturing Technology, 2009. 58(1): p. 181-184.
35. Li X.H., Wang Z.L., Zhao W.S., and Hu F.Q., *Pulsed micro electrochemical machining technology.* Key Engineering Materials 2007. 339: p. 327-331.
36. Kim B.H., Ryu S.H., Choi D.K., and Chu C.N., *Micro electrochemical milling.* Journal of Micromechanics and Microengineering, 2005. 15(1): p. 124-129.
37. Munda J. and Bhattacharyya B., *Investigation into electrochemical micromachining (EMM) through response surface methodology based approach.* The International Journal of Advanced Manufacturing Technology, 2006. 35(7-8): p. 821-832.
38. Smirnova L.V., Balmasov A.V., and Rumyantsev E.M., *Anodic behavior of tungsten in water – organic solutions of sodium chloride.* Russian Journal of Electrochemistry, 2000. 36(Volume 36, Number 7 / July): p. 712-715.
39. Masuzawa T., *Electrochemical Surface Finishing of Tungsten Carbide Alloy.* CIRP Annals - Manufacturing Technology, 1991. 40(1): p. 199-202.

40. Zhou C.D. and Taylor E.J., *Electrochemical machining for hard passive alloys with pulse reverse current.* Transactions of the NAMRI/SME 1997. 25: p. 147–152.
41. Masuzawa T., *A Combined Electrical Machining Process for Micronozzle Fabrication.* CIRP Annals - Manufacturing Technology, 1994. 43(1): p. 189-192.
42. Lim H., Wong Y., Rahman M., and Edwinlee M., *A study on the machining of high-aspect ratio micro-structures using micro-EDM.* Journal of Materials Processing Technology, 2003. 140(1-3): p. 318-325.
43. Zhu B.G. and Wang Z.L., *Fabrication of Microelectrode by Current Density Control in Electrochemical Micromachining.* Materials Science Forum 2006. 532-533 p. 221-224.
44. Wang Z.L. and Zhu B.G., *Method of Microelectrode with electrochemical machining and its applications.* Key Engineering Materials 2007. 339 p. 360-364.
45. Lim Y.M. and Kim S.H., *An electrochemical fabrication method for extremely thin cylindrical micropin.* Int J Mach Tools Manuf 2001. 41(15): p. 2287– 96.
46. Fan Z.W., Hourng L.W., and Wang C.Y., *Fabrication of tungsten microelectrodes using pulsed electrochemical machining.* Precision Engineering, 2010. 34(3): p. 489-496.
47. Jahan M.P., Rahman M., Wong Y.S., and Fuhua L., *On-machine fabrication of high-aspect-ratio micro-electrodes and application in vibration-assisted micro-electrodischarge drilling of tungsten carbide.* Proceedings of the Institution of Mechanical Engineers, Part B: Journal of Engineering Manufacture, 2010. 224(5): p. 795-814.
48. Rees A., Dimov S.S., Ivanov A., Herrero A., and Uriarte L.G., *Micro-EDM: factors affecting the quality of electrodes dressed on the machine.* Proc Inst Mech Eng, B J Eng Manuf 2007. 221(3): p. 409–418.
49. Ahn S., *Electro-chemical micro drilling using ultra short pulses.* Precision Engineering, 2004. 28(2): p. 129-134.
50. Wang M.H., Zhu D., and Peng W., *Experimental Research on Electrochemical Micromachining.* Advanced Design and Manufacture to Gain a Competitive Edge, 2008. Chapter 6: p. 775-783.
51. Chen H., Wang Z.L., Peng Z.L., Dong Y.H., and Zhao W.S., *Electrochemical Micro Machining of Stainless Steel with Voltage Pulses.* Advanced Materials Research, 2009. 69-70: p. 219-224.

52. Mujumdar, S.S., S.A. Mastud, R.K. Singh, and S.S. Joshi, *Experimental characterization of the reverse micro-electrodischarge machining process for fabrication of high-aspect-ratio micro-rod arrays.* Proceedings of the Institution of Mechanical Engineers, Part B: Journal of Engineering Manufacture, 2010. 224(5): p. 777-794.
53. Rajurkar K.P., Wei B., Kozak J., and McGeough J., *Modelling and Monitoring Interelectrode Gap in Pulse Electrochemical Machining.* CIRP Annals - Manufacturing Technology, 1995. 44(1): p. 177-180.
54. Kozak J., *Mathematical models for computer simulation of electrochemical machining processes.* Journal of Materials Processing Technology, 1998. 76: p. 170-175.
55. Kozak J., Dabrowski L., Lubkowski K., Rozenek M., and Slawinski R., *CAE-ECM system for electrochemical technology of parts and tools.* Journal of Materials Processing Technology, 2000. 107: p. 293-299.
56. Purcar M., Bortels L., Vandenbossche B., and Deconinck J., *3D electrochemical machining computer simulations.* Journal of Materials Processing Technology, 2004. 149(1-3): p. 472-478.
57. Kozak J., Gulbinowicz D., and Gulbinowicz Z., *The Mathematical Modeling and Computer Simulation of Pulse Electrochemical Micromachining.* Engineering Letter, 2008. 16: p. 556-561.
58. Ma N., Xu W., Wang X., and Tao B., *Pulse electrochemical finishing: Modeling and experiment.* Journal of Materials Processing Technology, 2010. 210(6-7): p. 852-857.
59. www.intellidrives.com. [cited 2011 01/11].
60. www.copleycontrols.com. [cited 2011 01/11].
61. Mathew R., James S., and Sundaram M.M., *Experimental Study of Micro Tools Fabricated by Electrochemical Machining.* Proc. of ASME International Manufacturing Science and Engineering Conference, 2010.

APPENDIX A: PUBLICATIONS / PRESENTATIONS

1. Mathew R., James S., Sundaram M.M., *Experimental Study of Micro Tools Fabricated by Electrochemical Machining.* Proc. of ASME International Manufacturing Science and Engineering Conference, 2010.
2. Research presentation on 'Experimental micromachining of High Aspect Ratio structures' at the 6th Annual Dayton Engineering Sciences Symposium (DESS), October 25th, 2010 at the Wright State University, Dayton, Ohio.
3. Mathew R., Sundaram M.M., *Fabrication of Ultra-High Aspect Ratio Metallic Micro Tools by Pulsed Electrochemical Micromachining* (to be submitted).

APPENDIX B : MATERIAL SAFETY DATA SHEETS

1. Sulphuric Acid

Common names

Sulphuric acid, vitriol, oil of vitriol

Chemical formula

H_2SO_4

Physical appearance

Form: Concentrated - colorless oily liquid, Dilute - colorless liquid

Stability: Stable, but hygroscopic.

Melting point: -2 °C

Water solubility: Miscible in all proportions (exothermic dissolution)

Specific gravity: 1.84 (concentrated), close to 1 (dilute)

Principal hazards

** Contact upon eyes or skin may cause serious permanent damage

** Concentrated solutions of acid are highly corrosive

** Dissolution of sulfuric acid in water is highly exothermic; enough release of heat to make water boil

Safe handling

Use of safety glasses. Avoid direct contact of acid or solution with skin. Dilution of acid to be done by skilled users. While diluting, eye protection is a must. Acid must be added to the water always, never the reverse way. Constant stirring is suggested as it prevents formation of a concentrated sulphuric acid layer at the bottom of the beaker. Also, the freshly prepared solution is hot and must be handled with extra care.

Case of Emergency

Eye contact: Flushing of eyes with water for at least 10 minutes. Must call for immediate medical help.

Skin contact: Wash contact area with plenty of water and remove any contaminated clothing. If reddening of skin persists, call for medical help.

If swallowed: Plenty of water must be drunk. Must call for immediate medical help.

Disposal rules

Dilute sulphuric acid in small quantities can be disposed down a sink with large quantitites of water unless prohibited by local rules. Larger amounts must be neutralized before disposal. Concentrated acid must never be disposed down a sink.

Protective equipment

Use of safety glass during handling of sulphuric acid or its solutions is a must. For concentrations upto 70%, materials of gloves include neoprene, natural rubber and PVC. For concentrated sulphuric acid, butyl rubber and polyethylene materials for gloves are suggested.

2. Sodium Chloride

Common names

Sodium chloride, common salt, table salt, sea salt, rock salt

Chemical formula

$NaCl$

Physical appearance

Form: White crystalline solid

Stability: Stable

Melting point: 804 °C

Boiling point: 1413 °C

Water solubility: substantial, colourless

Specific gravity: 2.16

Principal hazards

** Contact upon eyes may cause irritation

Safe handling

Use of safety glasses if required by local rules.

Case of Emergency

Eye contact: Flushing of eyes with water.

Disposal Rules

Sodium chloride may be disposed of in the sink in small quantities.

Protective equipment

Use of safety glasses as required by the local rules.